

Basis-independent stabilizerness and maximally noisy magic states

Michael Zurel^{1,*} and Jack Davis^{2,†}

¹*Department of Mathematics, Simon Fraser University, Burnaby, Canada*

²*DIENS, École Normale Supérieure, PSL University,*

CNRS INRIA, 45 rue d'Ulm, Paris 75005, France

(Dated: February 27, 2026)

Absolutely stabilizer states are those that remain convex mixtures of stabilizer states after conjugation by any unitary. Here we give a characterization of such states for multiple qudits of all prime dimensions by introducing a polytope of their allowed spectra. We illustrate this through the examples of one qubit, two qubits, and one qutrit. In particular, the set of absolutely stabilizer states for a single qubit is a ball inscribed in the stabilizer octahedron, but for higher dimensions the geometry is more complicated. For odd-prime-dimensional qudits, we also give a complete characterization of absolutely Wigner-positive states, i.e., states whose Wigner function remains nonnegative after conjugation by any unitary. In so doing, we show there are absolutely Wigner-positive states that are not absolutely stabilizer, which can be seen as a unitarily-invariant version of bound magic. We then study the radii of the largest balls contained in the sets of absolutely stabilizer states and absolutely Wigner-positive states. These radii respectively tell us the lowest possible purity of nonstabilizer and Wigner-negative states. Conversely, we also find the radius of the smallest ball containing the set of absolutely Wigner-positive states, giving a tight purity-based necessary condition thereof.

I. INTRODUCTION

Stabilizer states are of fundamental importance in quantum computation. They provide the structural foundation upon which much of the field rests, and are indispensable in the sub-fields of quantum error correction and classical simulation [1–8]. Such states define the complementary set of non-stabilizer, or magic states, as those inexpressible as a convex mixture of pure stabilizer states. Classifying, manipulating, and distilling such magic states is essential for achieving universality in the gate-injection model of fault-tolerant quantum computation [9–15]. Consequently, characterizing the structure and geometry of mixed stabilizer states is central for understanding the onset of quantum advantage.

The property of a state being stabilizer or non-stabilizer is inherently basis-dependent: a stabilizer state with respect to the computational basis can be a magic state in another basis. This is an immediate consequence of the unitary group acting transitively on pure states, with a prototypical example being the non-Clifford T gate mapping the stabilizer state $|+\rangle$ into the magic state $|T\rangle$. While the fault-tolerant implementation of such a unitary is highly constrained by the Eastin-Knill theorem [16], this observation nonetheless suggests an important question: which mixed quantum states remain stabilizer under arbitrary unitary conjugation? Having a characterization of such a set is highly desirable as it would allow one to test if a given state is stabilizer given only its set of eigenvalues.

Motivated by recent work implying the existence of such *absolutely stabilizer* states via fidelity-based magic

detection [17], here we provide a systematic characterization of the set of absolutely stabilizer states, which we also dub the *muggle set*. Our main result is showing that membership is governed by linear inequalities on the spectrum of a given state. In particular, we show that beyond the single-qubit case, the set of absolutely stabilizer states is not the inscribed ball of the stabilizer polytope, nor any other Hilbert-Schmidt ball in the space of Hermitian operators. Even for the cases of a single qutrit and two qubits, counterexamples can be constructed. This is because the purity no longer determines the spectrum of a state uniquely, implying that the subset of fixed-purity states decomposes into disjoint unitary orbits. Consequently, any unitarily-invariant set, including in particular the muggle set, need not coincide with a Hilbert-Schmidt ball. Note that our usage of unitarily invariance objects differs from [18], which focuses on sets of states rather than individual ones.

Our main technical approach is to analyze the polar dual of the stabilizer polytope, called the Λ polytope, where vertices of the former correspond to facets of the latter, and vice-versa [19–21]. In the unitarily-invariant setting of absolutely stabilizer states, we derive a criterion relating a state's spectrum and the spectra of the vertices of Λ . The result is a polytope in the simplex of state spectra, which we call the *absolutely stabilizer spectral polytope*, or *muggle polytope* for short. The absolutely stabilizer states are then those with spectra in this polytope.

In the context of multi-qubit systems, we then exploit the structure of the Λ polytope using the closed and non-contextual (CNC) framework [22] to dramatically reduce the number of vertices that must be evaluated to test if a given state is absolutely stabilizer. This leads to a natural conjecture, which we analytically verify for low-dimensional examples and give supporting numerical evidence in higher dimensions. In the two-qubit case, this

* mzurel@sfu.ca

† jack.davis@inria.fr

refinement is provably optimal and realizes the muggle polytope as having exactly 18 facets, a reduction in redundancy from 22,320 vertices of Λ .

Using similar techniques, we go on to analyze the Hilbert-Schmidt inradius of the stabilizer polytope, i.e., the radius of the largest Hilbert-Schmidt ball contained in the polytope. This radius depends strongly on whether the local dimension is even or odd, which we find to be a consequence of the existence of state-independent proofs of contextuality using multiqubit Pauli operators [23], which don't exist in odd dimensions [24, 25]. For odd-prime dimensions we derive the inradius exactly, while for qubits the radius we find relies on a conjecture about the structure of the Λ polytope. Our conjecture exactly matches that of Conjecture 1 in the recent work [17], offering a different perspective via the framework of closed and noncontextual sets of Pauli operators.

Finally, we discuss the related notion of absolute Wigner positivity (AWP) in odd-prime dimensions [26]; see also [27, 28]. Such states are those whose Wigner function [29–31] remains nonnegative under arbitrary unitary conjugation. Our techniques for characterizing the spectra carry over directly to the AWP setting, which yields the *AWP polytopes* in the simplex of spectra. Similar polytopes have been constructed for other kinds of Wigner functions [27, 28], but here we study them for the Wigner function most common to quantum computation [29–31]. This object is more tractable than the muggle polytope due to relative simplicity of the Wigner polytope (i.e. the convex hull of the phase space point operators) as compared to the stabilizer polytope. We find that the AWP set is similarly not the Hilbert-Schmidt inball of the Wigner polytope, and moreover that in the case of a single qutrit the muggle polytope is a strict subset of the AWP polytope. That is, there exist mixed qutrit states that are non-stabilizer yet no global unitary can generate negativity. This inclusion of spectral polytopes can be seen as a unitarily-invariant version of bound magic [32]; see also [33, 34]. Finally, we show that the inball of the Wigner polytope matches the inball of the stabilizer polytope in odd-prime dimensions.

The rest of the article is organized as follows. In Section II we recall the relevant background, including the stabilizer subtheory, the Wigner function, and the framework of closed and noncontextual sets of Pauli operators. Section III then presents our spectral characterization of absolutely stabilizer states, and we illustrate this characterization through some examples. In Section IV, we fully characterize the set of absolutely Wigner positive states. Finally, in Section V we find the radii of the largest ball contained in the sets of absolutely stabilizer and absolutely Wigner positive states, and we compare these radii against other related radii. Section VI concludes with a discussion of our results.

II. BACKGROUND

A. The stabilizer formalism

Here we recall certain aspects of the stabilizer formalism [1, 2, 21, 30, 35–38]. While some of the following definitions and statements are valid in all n -qudit Hilbert spaces $\mathcal{H} \simeq (\mathbb{C}^d)^{\otimes n}$, we restrict attention throughout to prime qudit dimension d .

The qudit Pauli X and Z operators for a single qudit ($n = 1$) are defined by their action on the computational basis $|j\rangle$,

$$X|j\rangle = |j+1\rangle, \quad Z|j\rangle = \omega^j|j\rangle, \quad \forall j \in \mathbb{Z}_d := \mathbb{Z}/d\mathbb{Z}, \quad (1)$$

where the arithmetic inside a ket is modulo d and $\omega = e^{2\pi i/d}$ is the first primitive d^{th} root of unity. For a system of n qudits these are used to build the set of discrete-variable displacement operators, here called generalized Pauli operators. These are labeled by vectors of the vector space $\mathbb{Z}_d^n \times \mathbb{Z}_d^n \simeq \mathbb{Z}_d^{2n} \simeq (\mathbb{Z}_d \times \mathbb{Z}_d)^{\times n}$. In particular, for $u = (u_z, u_x) \in \mathbb{Z}_d^n \times \mathbb{Z}_d^n$, the generalized Pauli operator is

$$T_u := \tau^{-u_z \cdot u_x} \bigotimes_{k=1}^n Z^{[u_z]_k} X^{[u_x]_k}, \quad (2)$$

where $\tau = (-1)^d e^{i\frac{\pi}{d}}$ [36]. The *Pauli group* is the group generated by the generalized Pauli operators, $\mathcal{P} = \langle \{T_a \mid a \in \mathbb{Z}_d^{2n}\} \rangle$, and the *Clifford group*, $\mathcal{C}\ell$, is the normalizer of the Pauli group with respect to the unitary group $U(d^n)$ modulo phases. The centre of the Pauli group $\mathcal{Z}(\mathcal{P})$ is isomorphic to the additive group \mathbb{Z}_d for odd d and to \mathbb{Z}_4 for $d = 2$, but in all cases $\mathcal{P}/\mathcal{Z}(\mathcal{P}) \simeq \mathbb{Z}_d^{2n}$.

The vector space \mathbb{Z}_d^{2n} is equipped with the standard symplectic form

$$[u, v] := u_z \cdot v_x - u_x \cdot v_z \pmod{d}, \quad (3)$$

which computes the group commutator between pairs of Pauli operators,

$$[T_u, T_v] := T_u T_v T_u^{-1} T_v^{-1} = \omega^{[u, v]} \mathbb{I}. \quad (4)$$

A subspace $I \subset \mathbb{Z}_d^{2n}$ over which the symplectic form vanishes is called *isotropic*, while an isotropic subspace of dimension n , which is the maximal dimension possible for such subspaces, is called *Lagrangian*. Isotropic subspaces are in one-to-one correspondence with equivalence classes of abelian subgroups of \mathcal{P} up to phases. Bases of a fixed isotropic subspace are in correspondence with generating sets of the associated abelian subgroup, again up to phases.

We also define a \mathbb{Z}_d -valued function β that tracks how *commuting* Pauli operators compose through the relation

$$T_u T_v = \omega^{-\beta(u, v)} T_{u+v}, \quad (5)$$

for all $u, v \in \mathbb{Z}_d^{2n}$ such that $[u, v] = 0$. With the phase convention chosen above in Eq. (2), the odd-dimensional

case reduces to $T_u T_v = \omega^{[u,v] \cdot 2^{-1}} T_{u+v}$, and so $\beta \equiv 0$. For qubits this is no longer the case, and, in fact, no phase prefactor replacing the one in Eq. (2) exists that can make $\beta \equiv 0$ for qubits [25].

This has important consequences for sets of commuting Pauli operators, which can be measured simultaneously. In particular, if a measurement of commuting operators T_u and T_v is performed yielding outcomes ω^a and ω^b respectively, the outcome ω^c for the measurement of observable T_{u+v} is uniquely determined via the operator relation

$$\omega^{-a-b} T_u T_v = \omega^{-a-b-\beta(u,v)} T_{u+v} = \omega^{-c} T_{u+v}. \quad (6)$$

More generally, if a set of commuting Paulis $\{T_{u_i}\}_{u_i \in \mathbb{Z}_d^{2n}}$ are measured yielding outcomes $\{\omega^{r(u_i)}\}_{u_i}$, the outcomes for the isotropic subspace $I := \langle u_1, u_2, \dots \rangle$ generated by these elements are fully determined. Therefore, we can label a measurement by an isotropic subspace I and a set of measurement outcomes via a function $r : I \rightarrow \mathbb{Z}_d$ satisfying consistency conditions like Eq. (6) for all pairs in I . Equivalently, with Eq. (5), r satisfies

$$r(u) + r(v) = r(u+v) - \beta(u,v) \quad \forall u, v \in I. \quad (7)$$

Hence assigning measurement outcomes to a collection of commuting Pauli operators is not always linear over an isotropic basis. For such a pair (I, r) , the corresponding projector is

$$\Pi_I^r = \frac{1}{|I|} \sum_{u \in I} \omega^{-r(u)} T_u. \quad (8)$$

In the case where $I = L$ is a Lagrangian subspace, the projector Π_L^r is rank one and can be identified with a pure quantum state, this is a pure stabilizer state. In fact, the set of all pure stabilizer states $|L, r\rangle\langle L, r|$ can be identified with such pairs (L, r) .

B. The stabilizer and Λ polytopes

We write $\text{Herm}(\mathcal{H})$ for the real vector space of Hermitian operators on the Hilbert space $\mathcal{H} \simeq (\mathbb{C}^d)^{\otimes n}$, while $\text{Herm}_c(\mathcal{H})$ denotes the affine subspace of $\text{Herm}(\mathcal{H})$ defined by $\text{Herm}_c(\mathcal{H}) := \{X \in \text{Herm}(\mathcal{H}) \mid \text{Tr}(X) = c\}$. Let \mathcal{S} denote the set of pure n -qudit stabilizer states. The *stabilizer polytope* is the convex hull of pure stabilizer state projectors,

$$\text{STAB} := \text{Conv}(\{|\sigma\rangle\langle\sigma| \mid |\sigma\rangle \in \mathcal{S}\}). \quad (9)$$

Any element of STAB is often referred to as a stabilizer state, and the abstract property of membership is sometimes called stabilizerness. The n -qudit Λ *polytope* is

$$\Lambda := \left\{ X \in \text{Herm}_1(\mathcal{H}) \mid \text{Tr}(X |\sigma\rangle\langle\sigma|) \geq 0 \quad \forall |\sigma\rangle \in \mathcal{S} \right\}. \quad (10)$$

These polytopes have many applications, including being used to define classical simulation algorithms for quantum computation [13, 20, 21] and to characterize magic state distillation [39].

Both STAB and Λ live in the affine space $\text{Herm}_1(\mathcal{H})$ of unit-trace Hermitian matrices. It will sometimes be convenient to translate these polytopes to the traceless subspace $\text{Herm}_0(\mathcal{H})$, the generalization of Bloch space

$$\text{STAB}_0 := \left\{ X - \frac{1}{d^n} \mathbb{I} \mid X \in \text{STAB} \right\}, \quad (11)$$

and

$$\Lambda_0 := \left\{ X - \frac{1}{d^n} \mathbb{I} \mid X \in \Lambda \right\}. \quad (12)$$

With respect to the Hilbert-Schmidt inner product, $\langle X, Y \rangle = \text{Tr}(XY)$, Λ_0 is the polar dual of $-d^n \text{STAB}_0$. That is,

$$\begin{aligned} \Lambda_0 &= (-d^n \text{STAB}_0)^\circ \\ &= \{X \in \text{Herm}_0(\mathcal{H}) \mid \text{Tr}(XY) \leq 1 \quad \forall Y \in -d^n \text{STAB}_0\}. \end{aligned} \quad (13)$$

C. The Wigner function

The Wigner function is a quasiprobability representation that describes quantum states, transformations, and measurements as real-valued functions over \mathbb{Z}_d^{2n} . Here we use the well-studied variant, valid in at least odd-prime dimensions, where negativity therein is linked to quantum contextuality and Wigner-positive circuits can be efficiently simulated on a classical computer [29–32, 40–42]. It arises via an operator basis known as the displaced parity basis or the set of *phase space point operators*. First define the multi-qudit parity operator as an expansion in the computational basis

$$A_0 := \sum_{j \in \mathbb{Z}_d^n} |-j\rangle\langle j| = \frac{1}{d^n} \sum_{u \in \mathbb{Z}_d^{2n}} T_u, \quad (14)$$

where again arithmetic inside kets is modulo d . The remaining phase space point operators are displaced versions thereof:

$$A_u = T_u A_0 T_u^\dagger \in \text{Herm}_1(\mathcal{H}), \quad \forall u \in \mathbb{Z}_d^{2n}. \quad (15)$$

These operators are Hermitian, have unit trace, and form an orthogonal basis in the space of operators, satisfying the orthogonality relation $\text{Tr}(A_u A_v) = d^n \delta_{u,v}$.

The Wigner function, $W_\rho : \mathbb{Z}_d^{2n} \rightarrow \mathbb{R}$, of a state ρ is given by the expansion coefficients of a state in this basis,

$$\rho = \sum_{v \in \mathbb{Z}_d^{2n}} W_\rho(v) A_v, \quad (16)$$

which, by orthogonality, can be extracted via

$$W_\rho(u) = \frac{1}{d^n} \text{Tr}(\rho A_u). \quad (17)$$

The *Wigner polytope*, denoted WP, is the set of Hermitian operators with nonnegative Wigner function. By orthogonality of the phase space point operators and the two descriptions of the Wigner function, Eq. (16) and Eq. (17), WP has dual descriptions: (1) as the convex hull of the phase space point operators

$$\text{WP} = \text{Conv}(\{A_u \mid u \in \mathbb{Z}_d^{2n}\}), \quad (18)$$

and (2) as an intersection of halfspaces

$$\text{WP} = \{X \in \text{Herm}_1(\mathcal{H}) \mid \text{Tr}(XA_u) \geq 0 \forall u \in \mathbb{Z}_d^{2n}\}. \quad (19)$$

Using a similar argument as in the previous subsection, this makes WP_0 the polar dual of $-d^n \text{WP}_0$ with respect to the Hilbert-Schmidt inner product.

A *Wigner-positive* state is one whose Wigner function is everywhere nonnegative: $W_\rho(u) \geq 0$ for all $u \in \mathbb{Z}_d^{2n}$ (we follow convention and do not refer to such states as Wigner-nonnegative). The set of Wigner-positive states is the intersection of the Wigner polytope with the set of quantum states. This is known to be a strict superset of the stabilizer polytope, a phenomenon known as *bound magic* [32]. See also [33, 34] for related notions of bound magic.

D. CNC operators

Closed and noncontextual (CNC) operators were introduced in Ref. [22] in order to define a quasiprobability function for qubits that is useful for simulating quantum computations, similar to the Wigner function for odd-dimensional qudits [32, 40]. They are defined with respect to certain sets of Pauli observables which do not contain state-independent proofs of contextuality like the Mermin square [23].

Definition 1. A set $\Omega \subset \mathbb{Z}_d^{2n}$ is closed under inference if for all $u, v \in \Omega$,

$$[u, v] = 0 \implies u + v \in \Omega. \quad (20)$$

In terms of observables, a set Ω is closed under inference if for any two commuting Pauli operators T_u and T_v with $u, v \in \Omega$, the vector $u + v$ corresponding to the product of the Pauli operators, $T_u T_v \propto T_{u+v}$, is also in Ω . The idea is, if T_u and T_v commute, and measurement outcomes of T_u and T_v are known, then the outcome of a measurement of T_{u+v} could be inferred. Closure under inference is also called partial closure in Ref. [43].

Definition 2. Let $\Omega \subset \mathbb{Z}_d^{2n}$ be a set that is closed under inference. A noncontextual value assignment for Ω is a function $\gamma : \Omega \rightarrow \mathbb{Z}_d$ such that for all $u, v \in \Omega$ with $[u, v] = 0$,

$$\gamma(u) + \gamma(v) = \gamma(u + v) - \beta(u, v). \quad (21)$$

Such a value assignment can be seen as a generalization of the above stabilizer consistency relation Eq. (7) from isotropic subspaces to sets that are closed under inference.

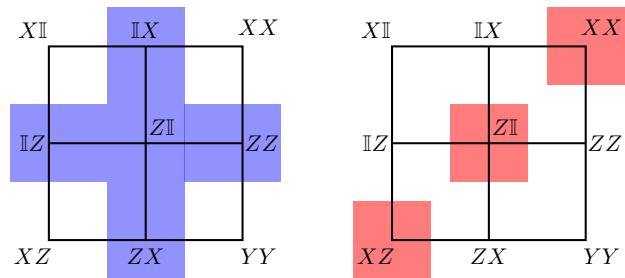


FIG. 1. CNC sets cannot contain observables forming a Mermin square-style proof of contextuality. (a) A subset of an $m = 1$ CNC set, and (b) a subset of an $m = 2$ CNC set on two qubits (see Theorem 1). In both cases, the Mermin square proof is avoided.

Definition 3. A set $\Omega \subset \mathbb{Z}_d^{2n}$ is noncontextual if there exists a noncontextual value assignment function $\gamma : \Omega \rightarrow \mathbb{Z}_d$.

A set $\Omega \subset \mathbb{Z}_d^{2n}$ that is both closed under inference and noncontextual is called CNC. A CNC operator is defined as follows.

Definition 4. For a pair (Ω, γ) where $\Omega \subset \mathbb{Z}_d^{2n}$ is CNC and $\gamma : \Omega \rightarrow \mathbb{Z}_d$ is a noncontextual value assignment for Ω , the corresponding CNC operator is

$$A_\Omega^\gamma = \frac{1}{d^n} \sum_{v \in \Omega} \omega^{-\gamma(v)} T_v. \quad (22)$$

The CNC sets $\Omega \subset \mathbb{Z}_d^{2n}$ and noncontextual value assignments $\gamma : \Omega \rightarrow \mathbb{Z}_d$ have been characterized for qudits of all prime dimensions [22, 44]. The characterization looks different for qubits than for odd-prime-dimensional qudits.

1. Qubits

Not every set of multiqubit Pauli observables is noncontextual because of the existence of Mermin square-style proofs of contextuality [23]. Intuitively, a CNC set is simply a collection of multiqubit Pauli observables that does not contain a state-independent proof of contextuality. In fact, if a set is closed under inference, then for it to be noncontextual, it suffices that it does not contain a set of operators with the same commutation relations as the nine Mermin square observables [20, Supplementary Material, Lemma 3] (see Figure 1 for some examples). With this condition, the multiqubit CNC sets can be fully characterized and classified. This is achieved by the following theorem.

Theorem 1 ([22]; §IV). A set $\Omega \subset \mathbb{Z}_2^{2n}$ is CNC if and only if it has the form

$$\Omega = \bigcup_{k=1}^{\xi} \langle a_k, I \rangle, \quad (23)$$

where $I \subset \mathbb{Z}_2^{2n}$ is an $(n - m)$ -dimensional isotropic subspace for some $m \in \{1, \dots, n\}$, $1 \leq \xi \leq 2m + 1$, $\{a_k\}_k$ pairwise anticommute, and all a_k commute with every element of I . Further, a CNC set is inclusion-maximal if and only if $\xi = 2m + 1$.

To get any noncontextual value assignments γ on a CNC set $\Omega \subset \mathbb{Z}_2^{2n}$, we can choose the values of γ freely on a basis for the subspace I , and on the elements a_1, \dots, a_ξ . Then the values assigned to the remaining elements of Ω can be inferred using Eq. (21). This characterization of the multiqubit CNC pairs (Ω, γ) is equivalent to the following characterization of the multiqubit CNC operators.

Corollary 1. *For any CNC set $\Omega \subset \mathbb{Z}_2^{2n}$ and any non-contextual value assignment $\gamma : \Omega \rightarrow \mathbb{Z}_2$, the corresponding CNC operator has the form*

$$A_\Omega^\gamma = g \left(A_{\tilde{\Omega}}^{\tilde{\gamma}} \otimes |\sigma\rangle\langle\sigma| \right) g^\dagger, \quad (24)$$

where $|\sigma\rangle$ is an $(n - m)$ -qubit stabilizer state, g is a n -qubit Clifford group element, and the nonzero vectors in the CNC set $\tilde{\Omega}$ pair-wise anticommute.

Since there are no nontrivial constraints imposed by Eq. (21) on the value assignment $\tilde{\gamma} : \tilde{\Omega} \rightarrow \mathbb{Z}_2$, the value of $\tilde{\gamma}$ can be chosen freely on the nonzero elements of $\tilde{\Omega}$.

For every number of n of qubits, CNC operators A_Ω^γ corresponding to maximal CNC sets Ω are vertices of the Λ polytopes [20, Supplementary Material, Sec. IV]. On n qubits, there are n orbits of CNC-type vertices of Λ under the action of the Clifford group. They are labeled by the parameter m , which takes integer values between 1 and n and determines the size and commutation structure of the CNC set via Theorem 1.

2. Odd-prime-dimensional qudits

In contrast to the qubit case, with odd-prime-dimensional qudits there are no state-independent proofs of contextuality among the Pauli operators [24, 25], so a set $\Omega \subset \mathbb{Z}_d^{2n}$ being CNC is equivalent to it being closed under inference. The CNC pairs (Ω, γ) have also been characterized for odd-prime dimensional qudits.

Theorem 2 ([44]; Theorem 1). *A set $\Omega \subset \mathbb{Z}_d^{2n}$ is closed under inference if and only if*

- (i) Ω is a subspace of \mathbb{Z}_d^{2n} (i.e., Ω is closed under addition), or
- (ii) Ω has the form

$$\Omega = \bigcup_{k=1}^{\xi} \langle a_k, I \rangle \quad (25)$$

where I is an $(n - m)$ -dimensional isotropic subspace of \mathbb{Z}_d^{2n} for some $m \in \{1, \dots, n\}$, $\{a_k\}_k$ pairwise do not commute, and all a_k commute with every element of I .

Unlike the qubit case, here the maximum value of ξ in Eq. (25) is not known [45].

One example of a maximal CNC set is the set $\Omega = \mathbb{Z}_d^{2n}$ of all Pauli operators. For multiple qudits ($n \geq 2$), the noncontextuality condition, Eq. (21), is enough to force the noncontextual value assignments, $\gamma : \mathbb{Z}_d^{2n} \rightarrow \mathbb{Z}_d$, to be linear functions [42]. The corresponding CNC operators, Eq. (22), are exactly the phase space point operators of the Wigner function [29, 30, 42, 46]. These operators are vertices of the multi-qudit Λ polytopes for every number of qudits [21, Theorem 3].

For a single qudit ($n = 1$), the situation is different. Since the noncontextuality condition does not impose linearity of the value assignment on all of \mathbb{Z}_d^{2n} , but only on commuting pairs of elements in \mathbb{Z}_d^{2n} , there exist CNC pairs $(\mathbb{Z}_d^{2n}, \gamma)$ where γ is non-linear. There are d^2 CNC operators corresponding to Wigner function phase space points, but there are another $d^{d+1} - d^2$ CNC operators corresponding to nonlinear value assignments on \mathbb{Z}_d^{2n} . For a single-qudit, these are also vertices of Λ , and in fact, all of the single-qudit Λ -polytope vertices are CNC operators with $\Omega = \mathbb{Z}_d^{2n}$. There are also CNC pairs (Ω, γ) with non-linear γ for multiple qudits, but only when $\Omega \subsetneq \mathbb{Z}_d^{2n}$ [44]. These are not known to be vertices of Λ in general.

III. ABSOLUTELY STABILIZER STATES

We now discuss our central topic of absolutely stabilizer states, beginning with their formal definition. We then derive our spectral characterization via a study of the Λ polytope. After separately specializing to qubits and odd-prime qudits, which are structurally different, we discuss the explicit cases of a single qubit, two qubits, and a single qudit.

A. Definition

Definition 5. *A state ρ is absolutely stabilizer if it remains a convex mixture of pure stabilizer states under arbitrary unitary conjugation,*

$$U\rho U^\dagger \in \text{STAB}, \quad \forall U \in \text{U}(d^n). \quad (26)$$

It immediately follows that the set of such states is the intersection of all unitarily transformed stabilizer polytopes,

$$\text{ASTAB} := \bigcap_{U \in \text{U}(d^n)} U \text{STAB} U^\dagger. \quad (27)$$

We also call ASTAB the *muggle set* and absolutely stabilizer states *muggle states*, which comes from the equivalent characterization of such states as those that cannot be transformed into any magic state with any unitary. The name *absolutely stabilizer* comes from the analogous

notion of absolute separability in the theory of entanglement [47] and in more general resource theories. The affinely shifted version is denoted

$$\begin{aligned} \text{ASTAB}_0 &= \text{ASTAB} - \frac{1}{d^n} \mathbb{I} \\ &= \bigcap_{U \in \text{U}(d^n)} U \text{STAB}_0 U^\dagger. \end{aligned} \quad (28)$$

Before characterizing the set of absolutely stabilizer states, we comment on a more general problem to illustrate why the problem is non-trivial. The shifted stabilizer polytope STAB_0 lives in the generalized Bloch space $\text{Herm}_0(\mathcal{H})$, which is a real Hilbert space with respect to the Hilbert-Schmidt inner product. Consider a subgroup G of the associated orthogonal group, $G \subset \text{O}(\text{Herm}_0(\mathcal{H}))$, and denote its action on matrices as $g(\cdot)$. The generalization of Eq. (28) becomes

$$\mathcal{O}_G := \bigcap_{g \in G} g(\text{STAB}_0). \quad (29)$$

If this group action was transitive on the Hilbert-Schmidt unit sphere, then clearly the intersection \mathcal{O}_G would be a Hilbert-Schmidt ball. In particular, it would be the inscribed ball of the stabilizer polytope. This happens for the single-qubit case because unitary conjugations are in one-to-one correspondence with Hilbert-Schmidt rotations. But for $d^n > 2$ this is no longer true: unitary conjugations preserve the entire spectrum of a Hermitian operator while Hilbert-Schmidt rotations only preserve the Euclidean norm of the spectrum (i.e. $\|A\|_2 = \sqrt{\text{Tr}(A^2)}$). More precisely, the set of unitary conjugations is a subgroup of orthogonal transformations,

$$\text{Ad}(\text{SU}(d^n)) \subset \text{O}(\text{Herm}_0(\mathcal{H})) \simeq \text{O}(d^{2n} - 1), \quad (30)$$

where $G = \text{Ad}(\text{SU}(d^n)) = \text{Ad}(\text{U}(d^n))$ is the image of the adjoint representation of the unitary group $\text{SU}(d^n)$ over $\text{Herm}_0(\mathcal{H}) \simeq \mathfrak{su}(d^n)$, seen as the Lie algebra $\mathfrak{su}(d^n)$.¹ Hence conjugate unitary action is not transitive on the Hilbert-Schmidt sphere, and so we cannot expect $\mathcal{O}_{\text{Ad}(\text{SU}(d^n))}$ to be a rescaled version thereof. In fact, since we are focusing on a subgroup of the rotation group we expect the muggle set to be a superset of the stabilizer inball:

$$\mathcal{O}_{\text{O}(\text{Herm}_0(\mathcal{H}))} \subset \mathcal{O}_{\text{Ad}(\text{SU}(d^n))} = \text{ASTAB}_0. \quad (31)$$

A useful (but slightly dangerous) visual analogy for seeing how lower symmetry implies a larger invariant set can be made for a single qubit by considering the intersection of all rotations of STAB_0 vs just the subgroup of z -axis rotations. The latter is clearly a superset of the former.

¹ We are using the physicist's version, $i\mathfrak{su}(d^n)$, without loss of generality.

B. Spectral characterization of absolutely stabilizer states

The set of absolutely stabilizer states is by definition unitarily-invariant. Membership of ASTAB is therefore determined only by the spectrum of a given state. In this section we show that ASTAB can be characterized as a polytope in the space of state spectra. We call such convex sets *absolutely stabilizer spectral polytopes*, or *muggle polytopes*. This characterization requires the following lemma relating the facets of the stabilizer polytope to the vertices of the Λ polytope.

Lemma 1. *For any $X \in \text{Herm}_1(\mathcal{H})$, $X \in \text{STAB}$ if and only if $\text{Tr}(XY) \geq 0$ for all vertices $Y \in \text{vert}(\Lambda)$.*

Proof of Lemma 1. For $X, Y \in \text{Herm}_1(\mathcal{H})$, we write

$$X = \frac{1}{d^n} \mathbb{I} + X_0 \quad \text{and} \quad Y = \frac{1}{d^n} \mathbb{I} + Y_0, \quad (32)$$

where $X_0, Y_0 \in \text{Herm}_0(\mathcal{H})$. Then the Hilbert-Schmidt inner product of X and Y is

$$\text{Tr}(XY) = \frac{1}{d^n} + \text{Tr}(X_0 Y_0). \quad (33)$$

Therefore, we have

$$\begin{aligned} &\{X \in \text{Herm}_1(\mathcal{H}) \mid \text{Tr}(XY) \geq 0 \forall Y \in \text{vert}(\Lambda)\} \\ &= \frac{1}{d^n} \mathbb{I} + \left\{ X_0 \in \text{Herm}_0(\mathcal{H}) \mid \begin{array}{l} -d^n \text{Tr}(X_0 Y_0) \leq 1 \\ \forall Y_0 \in \text{vert}(\Lambda_0) \end{array} \right\}. \end{aligned} \quad (34)$$

That this set is equal to STAB follows from the polar duality between Λ_0 and $-d^n \text{STAB}_0$, or equivalently from the polar duality between STAB_0 and $-d^n \Lambda_0$. More explicitly, the second term on the right hand side of Eq. (34) is the polar dual of the polar dual of STAB_0 , and so with the fact that STAB_0 contains the origin (since STAB contains the maximally mixed state), by a standard result in polytope theory this is equal to STAB [48, Theorem 2.11]. \square

We now arrive at the first result of this section: a characterization of the spectra of absolutely stabilizer states.

Theorem 3. *For any number of qudits n of any prime Hilbert space dimension d , an n -qudit state ρ is absolutely stabilizer if and only if*

$$\sum_{k=1}^{d^n} \lambda_k^\uparrow(\rho) \lambda_k^\downarrow(A) \geq 0 \quad \forall A \in \text{vert}(\Lambda), \quad (35)$$

where $\lambda^\uparrow(X)$ (resp. $\lambda^\downarrow(X)$) denotes the vector of eigenvalues of the operator X in non-decreasing (resp. non-increasing) order.

The proof relies on the following corollary of a theorem of Ky Fan [49, 50].

Corollary 2 (Ref. [51], Proposition 20.A.2.a). *If G is an $n \times n$ Hermitian matrix with eigenvalues $\lambda_1 \geq \dots \geq \lambda_n$, and H is an $n \times n$ Hermitian matrix with eigenvalues $\mu_1 \geq \dots \geq \mu_n$, then*

$$\max_{U \in \mathcal{U}(n)} \text{Tr}(UGU^\dagger H) = \sum_{i=1}^n \lambda_i \mu_i, \quad \text{and} \quad (36)$$

$$\min_{U \in \mathcal{U}(n)} \text{Tr}(UGU^\dagger H) = \sum_{i=1}^n \lambda_i \mu_{n-i+1}. \quad (37)$$

Proof of Theorem 3. Using Lemma 1 together with the definition of ASTAB, for a state ρ we know that $\rho \in \text{ASTAB}$ if and only if

$$\text{Tr}(U\rho U^\dagger A) \geq 0, \quad \forall A \in \text{vert}(\Lambda), \forall U \in \mathcal{U}(d^n). \quad (38)$$

For any given vertex A of Λ , the condition Eq (38) must hold for all unitaries $U \in \mathcal{U}(d^n)$. This is equivalent to the condition,

$$\min_{U \in \mathcal{U}(d^n)} \text{Tr}(U\rho U^\dagger A) \geq 0, \quad \forall A \in \text{vert}(\Lambda). \quad (39)$$

Then the theorem follows from Corollary 2 with $G = \rho$ a candidate absolutely stabilizer state and $H = A$ a vertex of Λ . \square

The conclusion of Theorem 3 is that the spectra of absolutely stabilizer states form a polytope contained in the unit simplex of possible state eigenvalues. The set of all absolutely stabilizer states is then the unitary group orbit of the diagonal matrices corresponding to these allowed spectra. This characterization however contains some redundancy. Namely, not all the vertices of Λ are needed. To determine which vertices of Λ contribute, we can use the theory of majorization [51]. We make the following definition.

Definition 6. *A subset $\mathcal{V}_{\text{sGen}} \subseteq \text{vert}(\Lambda)$ is spectrally generating if for every vertex $A \in \text{vert}(\Lambda)$ there exists a*

probability distribution $p(B|A)$ on $\mathcal{V}_{\text{sGen}}$ such that

$$\lambda^\downarrow(A) \preceq \sum_{B \in \mathcal{V}_{\text{sGen}}} p(B|A) \lambda^\downarrow(B). \quad (40)$$

That is, a subset of vertices is here said to be spectrally generating if the spectrum of any other vertex is majorized by a convex combination of the spectra of the given subset. To determine the allowed spectra of absolutely stabilizer states, we need only the constraints of the form Eq. (35) from a spectrally generating set of vertices.

Theorem 4. *Let $\mathcal{V}_{\text{sGen}} \subseteq \text{vert}(\Lambda)$ be spectrally generating in the sense of Definition 6. Then a state ρ is absolutely stabilizer if and only if*

$$\sum_{k=1}^{d^n} \lambda_k^\uparrow(\rho) \lambda_k^\downarrow(A) \geq 0 \quad \forall A \in \mathcal{V}_{\text{sGen}}. \quad (41)$$

Proof of Theorem 4. Fix a spectrally generating set $\mathcal{V}_{\text{sGen}} \subseteq \text{vert}(\Lambda)$. We want to show that the set of states defined by Eq. (41) is equal to the set of states defined by Eq. (35). That Eq. (35) implies Eq. (41) for any state ρ follows immediately from the inclusion $\mathcal{V}_{\text{sGen}} \subseteq \text{vert}(\Lambda)$.

For the opposite direction, suppose a state ρ satisfies Eq. (41). Consider an arbitrary vertex A of Λ . By assumption, there exists a probability distribution $p(B|A)$ on $\mathcal{V}_{\text{sGen}}$ such that

$$\lambda^\downarrow(A) \preceq \sum_{B \in \mathcal{V}_{\text{sGen}}} p(B|A) \lambda^\downarrow(B). \quad (42)$$

Let $\mu^\downarrow = \sum_B p(B|A) \lambda^\downarrow(B)$. Since ρ satisfies Eq. (41), we have

$$\sum_{k=1}^{d^n} \lambda_k^\uparrow(\rho) \mu_k^\downarrow = \sum_{B \in \mathcal{V}_{\text{sGen}}} p(B|A) \sum_{k=1}^{d^n} \lambda_k^\uparrow(\rho) \lambda_k^\downarrow(B) \geq 0. \quad (43)$$

Then, using summation by parts,

$$\sum_{k=1}^{d^n} \lambda_k^\uparrow(\rho) \lambda_k^\downarrow(A) = \lambda_{d^n}^\uparrow(\rho) \left(\underbrace{\sum_{\ell=1}^{d^n} \lambda_\ell^\downarrow(A)}_{=1} \right) - \sum_{k=1}^{d^n-1} \left(\underbrace{\sum_{\ell=1}^k \lambda_\ell^\downarrow(A)}_{\leq \sum_{\ell=1}^k \mu_\ell^\downarrow} \right) \underbrace{(\lambda_{k+1}^\uparrow(\rho) - \lambda_k^\uparrow(\rho))}_{\geq 0} \quad (44)$$

$$\geq \lambda_{d^n}^\uparrow(\rho) \left(\sum_{\ell=1}^{d^n} \mu_\ell^\downarrow \right) - \sum_{k=1}^{d^n-1} \left(\sum_{\ell=1}^k \mu_\ell^\downarrow \right) (\lambda_{k+1}^\uparrow(\rho) - \lambda_k^\uparrow(\rho)) = \sum_{k=1}^{d^n} \lambda_k^\uparrow(\rho) \mu_k^\downarrow \geq 0. \quad (45)$$

Here the first line is the summation by parts formula, the second line follows from the assumption $\lambda^\downarrow(A) \preceq \mu^\downarrow$ together with the relations indicated in the underbraces, and finally we apply the summation by parts formula in reverse. The last inequality was shown above. Therefore,

for any state ρ , Eq. (35) follows from Eq. (41). \square

The last piece of the characterization of the set of absolutely stabilizer states is a characterization of a spectrally generating vertices $\mathcal{V}_{\text{sGen}}$. Since the spectra of the ver-

tices of Λ are different for qubits than they are for odd-prime-dimensional qudits, here we split into two cases.

1. Qubits

The spectrum of a CNC-type vertex of Λ is determined by the parameter m described in Theorem 1. This is described by the following lemma.

Lemma 2. *For any number of qubits n and any $m \in \{1, \dots, n\}$, every n -qubit CNC operator A_Ω^γ correspond to a maximal CNC set Ω of type m has eigenvalues*

$$\begin{cases} \frac{1+\sqrt{2m+1}}{2^m} & \text{with multiplicity } 2^{m-1}, \\ \frac{1-\sqrt{2m+1}}{2^m} & \text{with multiplicity } 2^{m-1}, \\ 0 & \text{with multiplicity } 2^n - 2^m. \end{cases} \quad (46)$$

Proof of Lemma 2. A CNC operator A_Ω^γ of type m has the form

$$A_\Omega^\gamma = g(A_\Omega^{\tilde{\gamma}} \otimes |\sigma\rangle\langle\sigma|)g^\dagger, \quad (47)$$

where g is an n -qubit Clifford group element, $|\sigma\rangle$ is an $(n-m)$ -qubit stabilizer state, and $A_\Omega^{\tilde{\gamma}}$ is a CNC operator such that all Pauli operators labeled by $\Omega \setminus \{0\}$ pair-wise anti-commute. Conjugation by unitary operators do not change the spectrum, so it suffices to characterize CNC operators of the form $A_\Omega^{\tilde{\gamma}} \otimes |\sigma\rangle\langle\sigma|$. The eigenvalues are all products of the eigenvalues of $A_\Omega^{\tilde{\gamma}}$ and the eigenvalues of $|\sigma\rangle\langle\sigma|$. But $|\sigma\rangle\langle\sigma|$ is a projector onto a pure $(n-m)$ -qubit state, so it has eigenvalue 1 with multiplicity 1 and eigenvalue 0 with multiplicity $2^{n-m}-1$. Thus, $A_\Omega^{\tilde{\gamma}} \otimes |\sigma\rangle\langle\sigma|$ has eigenvalue 0 with multiplicity $2^m(2^{n-m}-1)$, and the remaining eigenvalues are exactly the eigenvalues of $A_\Omega^{\tilde{\gamma}}$.

The operator $2^m A_\Omega^{\tilde{\gamma}} - \mathbb{I}$ is a sum of pair-wise anticommuting Pauli operators (the non-identity Pauli operators in $\tilde{\Omega}$). We have

$$(2^m A_\Omega^{\tilde{\gamma}} - \mathbb{I})^2 = \left(\sum_{b \in \tilde{\Omega} \setminus \{0\}} (-1)^{\tilde{\gamma}(b)} T_b \right)^2 \quad (48)$$

$$= \sum_{b \in \tilde{\Omega} \setminus \{0\}} (-1)^{2\tilde{\gamma}(b)} T_b^2 \quad (49)$$

$$+ \sum_{\substack{a, b \in \tilde{\Omega} \setminus \{0\} \\ a \neq b}} (-1)^{\tilde{\gamma}(a) + \tilde{\gamma}(b)} T_a T_b \quad (50)$$

$$= |\tilde{\Omega} \setminus \{0\}| \mathbb{I} = (2m+1) \mathbb{I}. \quad (51)$$

The last term in the second line above vanishes as a result of the pair-wise anti-commutation of the operators in the set. Therefore, the eigenvalues of $2^m A_\Omega^{\tilde{\gamma}} - \mathbb{I}$ are in $\{-\sqrt{2m+1}, \sqrt{2m+1}\}$. Since $\text{Tr}(2^m A_\Omega^{\tilde{\gamma}} - \mathbb{I}) = 0$, each eigenvalue must appear with equal multiplicity. The result follows. \square

Not all vertices of Λ are of CNC type, but there is evidence that vertices of CNC type form a spectrally generating set in the sense of Definition 6. Therefore, we make the following conjecture.

Conjecture 1. *For any number of qubits and any vertex $A \in \text{vert}(\Lambda)$, the eigenvalues $\lambda^\downarrow(A)$ of A are majorized by a convex combination of the eigenvalues $\lambda^\downarrow(A_\Omega^\gamma)$ of CNC-type vertices of Λ .*

By directly enumerating the vertices of Λ for one and two qubits, we confirm the conjecture for these cases. This is shown in Appendix A, together with numerical evidence for this conjecture from higher numbers of qubits. If the conjecture is true, we obtain an especially clean spectral characterization of the multi-qubit muggle set.

Theorem 5. *If Conjecture 1 is true, then a multiqubit state ρ is absolutely stabilizer if and only if, for all $m \in \{1, \dots, n\}$,*

$$\frac{1 + \sqrt{2m+1}}{2^m} \sum_{k=1}^{2^{m-1}} \lambda_k^\uparrow(\rho) + \frac{1 - \sqrt{2m+1}}{2^m} \sum_{k=1}^{2^{m-1}} \lambda_k^\downarrow(\rho) \geq 0. \quad (52)$$

Proof of Theorem 5. This is the immediate conclusion of Theorem 4, Conjecture 1, and Lemma 2. \square

2. Odd-prime-dimensional qudits

There are two different classes of CNC operators for odd-prime-dimensional qudits, those with linear value assignments and those with nonlinear value assignments. The eigenvalues of the first class are described by the following lemma.

Lemma 3. *For any number n of qudits with odd-prime dimension d , the phase space point operators A_u of the Wigner function have eigenvalues*

$$\begin{cases} 1 & \text{with multiplicity } \frac{1}{2}(d^n + 1), \\ -1 & \text{with multiplicity } \frac{1}{2}(d^n - 1). \end{cases} \quad (53)$$

Proof of Lemma 3. The phase space point operator A_u , $u \in \mathbb{Z}_d^{2n}$ can be obtained from A_0 by $A_u = T_a A_0 T_a^\dagger$. Conjugation by unitary operators doesn't change the eigenvalues, so it suffices to characterize the eigenvalues of A_0 . It can easily be shown using Eq. (14) that the parity operator A_0 satisfies $A_0^2 = \mathbb{I}$. Therefore, the eigenvalues of A_u are in $\{-1, 1\}$. Since $\text{Tr}(A_u) = 1$, the multiplicity of eigenvalue +1 must be one more than the multiplicity -1. The result follows. \square

Through Eq. (35), this gives a necessary condition for an n -qudit state ρ to be an absolutely stabilizer state, namely,

$$\sum_{k=1}^{(d^n+1)/2} \lambda_k^\uparrow(\rho) - \sum_{k=1}^{(d^n-1)/2} \lambda_k^\downarrow(\rho) \geq 0. \quad (54)$$

Since the noncontextuality condition Eq. (21) enforces non-linearity only on *commuting* triples $u, v, u + v \in \Omega$, for odd-prime dimensional qudits there are CNC operators which are vertices of Λ but are not phase space point operators [21, 24, 44]. This can be seen already for a single qutrit. There, there are nine phase space point operators, but the Λ polytope has 81 vertices. The remaining 72 vertices are CNC operators with $\Omega = \mathbb{Z}_3^2$ and with non-linear value assignments γ [42].

We could make the same conjecture about CNC operators being a spectrally generating set, Conjecture 1, for odd-prime-dimensional qudits, and this would give us a similarly conditional characterization of the muggle set as Theorem 5. However, a complete classification of the spectra of multiqutrit CNC operators is currently not known. Even for a single-qutrit, there are many possible spectra of Λ polytope vertices. In this case, all vertices of Λ are CNC type, but there are many unitary group orbits of CNC-type operators. They are enumerated up to $d = 7$ in Ref. [52]. They find two orbits (i.e., two distinct spectra) for $d = 3$, 9 for $d = 5$, and 210 for $d = 7$. A complete characterization of CNC spectra on odd-prime-dimensional qudits is currently out of reach.

C. Examples

In this section, we illustrate the set of muggle states through three examples: (1) one qubit, (2) two qubits, and (3) one qutrit.

1. One qubit

The one-qubit case is easy to visualize. The set of physical states is the Bloch ball, a Hilbert-Schmidt ball in the 3-dimensional real affine space $\text{Herm}_1(\mathbb{C}^2)$. There are six pure stabilizer states, two eigenstates for each of the X , Y , and Z Pauli operators. These are the vertices of $\text{STAB} \subset \text{Herm}_1(\mathbb{C}^2)$, which forms a regular octahedron.

On a single-qubit, Λ is a cube with vertices $A_{\pm\pm\pm} = \frac{1}{2}(I \pm X \pm Y \pm Z)$. These vertices are all unitarily equivalent with eigenvalues $(1 \pm \sqrt{3})/2$. The set of absolutely stabilizer states consists of all states with eigenvalues $(1 - \lambda, \lambda)$, where without loss of generality we assume $1 - \lambda \geq \lambda$, satisfying

$$\begin{cases} \lambda, 1 - \lambda \geq 0 \\ \frac{1+\sqrt{3}}{2}\lambda + \frac{1-\sqrt{3}}{2}(1 - \lambda) \geq 0. \end{cases} \quad (55)$$

These constraints simplify to

$$\frac{1}{2} - \frac{1}{2\sqrt{3}} \leq \lambda \leq \frac{1}{2}, \quad (56)$$

corresponding to diagonal matrices $(\mathbb{I} + zZ)/2$ with $0 \leq z \leq 1/\sqrt{3}$. The set of all absolutely stabilizer states is the unitary orbit of these diagonal states. These are

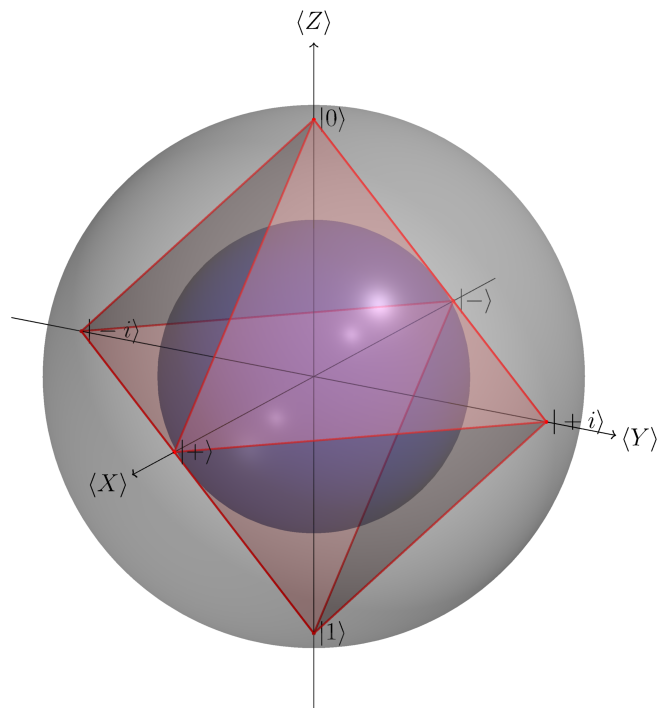


FIG. 2. The single-qubit Bloch ball is shown in gray containing the stabilizer octahedron in red and the set of single-qubit absolutely stabilizer states in blue. In the single-qubit case, the set of absolutely stabilizer states is a Hilbert-Schmidt ball inscribed in the stabilizer octahedron.

states of the form $\rho(x, y, z) = \frac{1}{2}(\mathbb{I} + xX + yY + zZ)$ with $x^2 + y^2 + z^2 \leq \frac{1}{3}$. This is simply a three-dimensional Hilbert-Schmidt ball in $\text{Herm}_0(\mathbb{C}^2)$, shifted to be centred at the maximally mixed state and inscribed in the stabilizer octahedron, the largest ball inscribed in the stabilizer polytope. This is illustrated in Figure 2.

2. Two qubits

The two-qubit stabilizer polytope is a 15-dimensional polytope with 60 vertices, corresponding to the 60 pure two-qubit stabilizer states. Λ has 22,320 vertices which fall into 8 orbits under the action of the Clifford group with 8 distinct spectra. Conjecture 1 holds in this case (this is shown in Appendix A), and so by Theorem 5 we only need the constraints from the spectra of the two unitary group orbits of CNC-type vertices. The spectra are

$$\lambda^\downarrow(A_\Omega^\gamma) = \begin{cases} \left(\frac{1+\sqrt{3}}{2}, 0, 0, \frac{1-\sqrt{3}}{2} \right) & \text{for } m = 1, \\ \left(\frac{1+\sqrt{5}}{4}, \frac{1+\sqrt{5}}{4}, \frac{1-\sqrt{5}}{4}, \frac{1-\sqrt{5}}{4} \right) & \text{for } m = 2. \end{cases} \quad (57)$$

Suppose the eigenvalues of a candidate absolutely stabilizer state ρ are $\lambda_1, \lambda_2, \lambda_3, \lambda_4$. Without loss of general-

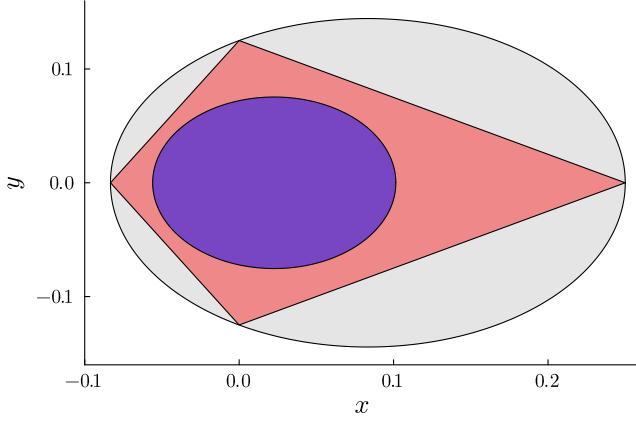


FIG. 3. Cross section of the set of 2-qubit states parametrized by $\rho(x, y) = \frac{1}{4}I + x(ZZ + XX - YY) + y(Z_1 + Z_2)$. The set of physical density matrices is shown in gray, STAB_0 in red, and ASTAB_0 in blue.

ity, we can assume the eigenvalues satisfy

$$\begin{cases} \lambda_1 \geq \lambda_2 \geq \lambda_3 \geq \lambda_4 \geq 0 \\ \lambda_1 + \lambda_2 + \lambda_3 + \lambda_4 = 1. \end{cases} \quad (58)$$

These constraints define the Weyl chamber: the sub-polytope in the of the three dimensional unit simplex of nonnegative spectra corresponding to spectra sorted in non-increasing order. Then, to get the allowed (sorted) spectra of absolutely stabilizer states, we impose the two additional constraints

$$\begin{cases} \frac{1-\sqrt{3}}{2}\lambda_1 + \frac{1+\sqrt{3}}{2}\lambda_4 \geq 0 \\ \frac{1-\sqrt{5}}{4}(\lambda_1 + \lambda_2) + \frac{1+\sqrt{5}}{4}(\lambda_3 + \lambda_4) \geq 0. \end{cases} \quad (59)$$

These constraints give us a three-dimensional polytope of allowed spectra with vertices.

$$\begin{cases} \left(\frac{1}{4}, \frac{1}{4}, \frac{1}{4}, \frac{1}{4} \right) \\ \left(\frac{5+\sqrt{3}}{22}, \frac{5+\sqrt{3}}{22}, \frac{5+\sqrt{3}}{22}, \frac{7-3\sqrt{3}}{22} \right) \\ \left(\frac{7+3\sqrt{3}}{22}, \frac{5-\sqrt{3}}{22}, \frac{5-\sqrt{3}}{22}, \frac{5-\sqrt{3}}{22} \right) \\ \left(\frac{5+\sqrt{5}}{20}, \frac{5+\sqrt{5}}{20}, \frac{5-\sqrt{5}}{20}, \frac{5-\sqrt{5}}{20} \right) \\ \left(\frac{5+\sqrt{5}}{20}, \frac{5+\sqrt{5}}{20}, \frac{5\sqrt{3}-4\sqrt{5}+\sqrt{15}}{20}, \frac{10-5\sqrt{3}+2\sqrt{5}-\sqrt{15}}{20} \right) \\ \left(\frac{10+5\sqrt{3}-2\sqrt{5}-\sqrt{15}}{20}, \frac{-5\sqrt{3}+4\sqrt{5}+\sqrt{15}}{20}, \frac{5-\sqrt{5}}{20}, \frac{5-\sqrt{5}}{20} \right) \end{cases} \quad (60)$$

The set of all unordered spectra is obtained by taking the convex hull of these 6 vertices together with all of their coordinate permutation. The result is a three-dimensional polytope of spectra with 40 vertices and 18 facets. The set of all absolutely stabilizer states is the set of all unitary conjugations of the diagonal matrices corresponding to these allowed spectra. A cross section of the 2-qubit state space, together with the stabilizer polytope and muggle set, is shown in Figure 3.

3. One qutrit

The single-qutrit stabilizer polytope has 12 vertices and 81 facets. The facets, which correspond to the 81 vertices of Λ , are all CNC-type, but they fall into two orbits under the action of the unitary group. 9 of them correspond to phase space point operators of the Wigner function (CNC operators $A_{\mathbb{Z}_d^2}^\gamma$ with linear value assignment γ), and the other 72 correspond to CNC operators with non-linear value assignments [42]. The eigenvalues of these operators are

$$\lambda^\downarrow \left(A_{\mathbb{Z}_3^2}^\gamma \right) = \begin{cases} (1, 1, -1) & \text{for linear } \gamma, \\ \left(\frac{1+\sqrt{5}}{2}, 0, \frac{1-\sqrt{5}}{2} \right) & \text{for nonlinear } \gamma. \end{cases} \quad (61)$$

Let $\lambda_1, \lambda_2, \lambda_3$ with $\lambda_1 \geq \lambda_2 \geq \lambda_3 \geq 0$ be the sorted eigenvalues of a candidate single-qutrit muggle state ρ . With non-negativity and normalization, $\lambda_1 + \lambda_2 + \lambda_3 = 1$, together with the constraints

$$\begin{cases} -\lambda_1 + \lambda_2 + \lambda_3 \geq 0, \\ \frac{1-\sqrt{5}}{2}\lambda_1 + \frac{1+\sqrt{5}}{2}\lambda_3 \geq 0, \end{cases} \quad (62)$$

from Theorem 4, we get a two-dimensional polygon of allowed ordered spectra for absolutely stabilizer states living in the Weyl chamber. Allowing unsorted spectra (i.e., coordinate permutations of the spectra in the Weyl chamber), we get the full polygon of allowed spectra living in the simplex of normalized nonnegative spectra. These absolutely stabilizer state spectra are shown in Figure 4. For comparison, Figure 4 also shows the allowed spectra of absolutely Wigner positive states [26] described in the next section.

IV. ABSOLUTE WIGNER POSITIVITY

On odd-prime-dimensional qudits, it is known that there are non-stabilizer states that cannot be distilled to useful magic states, and on which stabilizer circuits can be efficiently simulated classically. These so-called bound magic states are non-stabilizer states with positive Wigner function [32]. Measures of negativity in the Wigner function serve as monotones with respect to the resource theory of magic [12]. Therefore, with a similar motivation as absolutely stabilizer states, we can define absolutely Wigner-positive states as those for which the Wigner function remains nonnegative after conjugation by any unitary group element [26]. In this section, we get a complete spectral characterization of the set of AWP states using similar methods as those we used to characterize absolutely stabilizer states in Section III.

Definition 7. *An n -qudit state ρ is absolutely Wigner-positive (or AWP) if the Wigner function of $U\rho U^\dagger$ is nonnegative for all unitary operators $U \in \mathcal{U}(d^n)$.*

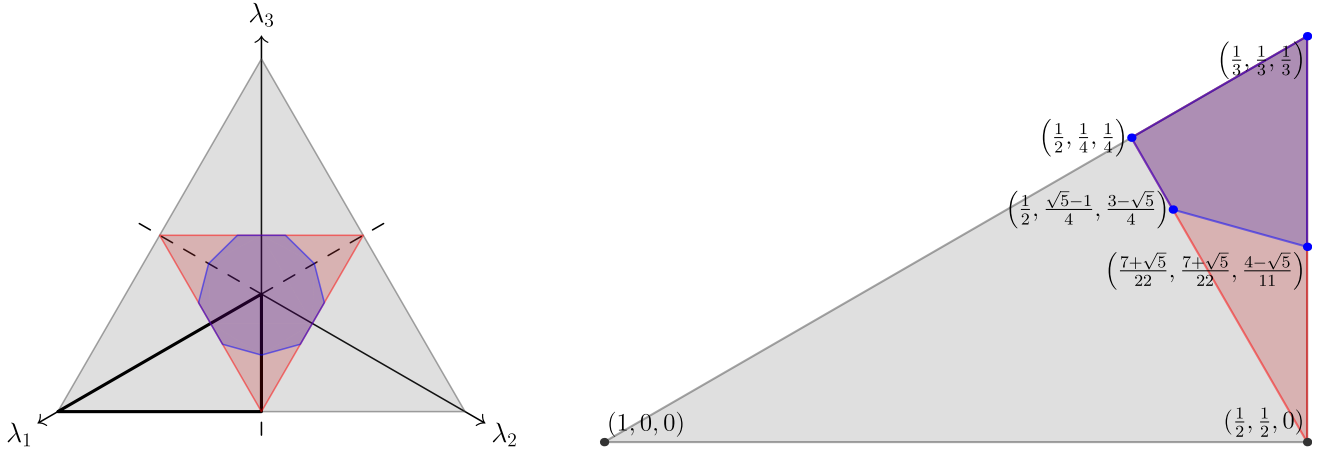


FIG. 4. Left: Ternary plot of the spectra of single-qudit absolutely stabilizer states (blue) and absolutely Wigner-positive states (red). Right: the associated Weyl chamber (i.e. the subset of ordered spectra) with special points of intersection displayed.

Similar to the description of the set of absolutely stabilizer states in Eq. (27), the set of absolutely Wigner-positive states, denoted AWP, is

$$\text{AWP} = \bigcap_{U \in \text{U}(d^n)} U \text{WP} U^\dagger. \quad (63)$$

This set is also unitarily-invariant and thus has a spectral characterization². With the following theorem, we get a complete characterization of the spectra of AWP states.

Theorem 6. *For any number of qudits n with odd-prime Hilbert space dimension d , an n -qudit state ρ is AWP if and only if*

$$\sum_{k=1}^{(d^n-1)/2} \lambda_k^\downarrow(\rho) \leq \frac{1}{2}, \quad (64)$$

i.e., the sum of the largest $(d^n - 1)/2$ eigenvalues of ρ is no more than $1/2$. Equivalently, a state ρ is AWP if and only if its spectrum is in the $d^n - 1$ -dimensional polytope formed by the convex hull of the vertices

$$\left\{ \begin{array}{l} \left(\underbrace{\frac{1}{d^n-1}, \dots, \frac{1}{d^n-1}}_{d^n-1 \text{ times}}, 0 \right) \\ \left(\frac{2}{d^n+1}, \underbrace{\frac{1}{d^n+1}, \dots, \frac{1}{d^n+1}}_{d^n-1 \text{ times}} \right) \end{array} \right. \quad (65)$$

and all of their coordinate permutations.

² Note that due to the size of the Wigner polytope, the set AWP as defined could *a priori* include non-positive-semi-definite operators. We show in the next section that this is not the case: all operators in AWP are positive semi-definite.

Proof of Theorem 6. With the description of the Wigner polytope Eq. (19), state ρ is AWP if and only if

$$\text{Tr}(U\rho U^\dagger A_u) \geq 0, \quad \forall u \in \mathbb{Z}_d^{2n}, \forall U \in \text{U}(d^n), \quad (66)$$

or equivalently,

$$\min_{U \in \text{U}(d^n)} \text{Tr}(U\rho U^\dagger A_u) \geq 0, \quad \forall u \in \mathbb{Z}_d^{2n}. \quad (67)$$

Using Corollary 2, together with Lemma 3 characterizing the eigenvalues of phase space point operators, we get the constraint that a state ρ is AWP if and only if

$$\sum_{k=1}^{(d^n+1)/2} \lambda_k^\uparrow(\rho) - \sum_{k=1}^{(d^n-1)/2} \lambda_k^\downarrow(\rho) \geq 0. \quad (68)$$

With normalization,

$$\sum_{k=1}^{d^n} \lambda_k^\downarrow(\rho) = \sum_{k=1}^{(d^n-1)/2} \lambda_k^\downarrow(\rho) + \sum_{k=1}^{(d^n+1)/2} \lambda_k^\uparrow(\rho) = 1, \quad (69)$$

Eq. (68) is equivalent to Eq. (64). This gives us the first statement of the theorem.

For the second statement of the theorem, let $\lambda_1, \dots, \lambda_{d^n}$ be the eigenvalues of an n -qudit candidate AWP state ρ . Without loss of generality, we can assume

$$\begin{cases} \lambda_1 \geq \lambda_2 \geq \dots \geq \lambda_{d^n} \geq 0, \\ \lambda_1 + \dots + \lambda_{d^n} = 1. \end{cases} \quad (70)$$

This gives us a Weyl chamber in the simplex of allowed spectra of physical quantum states. This Weyl chamber is a $d^n - 1$ -dimensional simplex in coordinates $(\lambda_1, \dots, \lambda_{d^n})$ defined by the constraints Eq. (70) and with vertices

$$\begin{cases} v_1 = (1, 0, \dots, 0), \\ v_2 = (\frac{1}{2}, \frac{1}{2}, 0, \dots, 0) \\ \vdots \\ v_{d^n} = (\frac{1}{d^n}, \dots, \frac{1}{d^n}). \end{cases} \quad (71)$$

The allowed spectra of AWP states in this Weyl chamber are obtained by imposing the additional inequality Eq. (64). Then, through one step of the double-description method for polytope vertex enumeration [53], we get the allowed AWP spectra. We will find the vertices of the subpolytope of the Weyl chamber obtained by imposing Eq. (64), and then show that after allowing unordered spectra (coordinate permutations of the spectra in the Weyl chamber), most of these vertices are redundant.

According to the double description method, the vertices of the new polytope obtained after imposing Eq. (64) on the Weyl chamber simplex have vertices consisting of (1) the Weyl chamber vertices which are consistent with this inequality, and (2) the intersection points of the hyperplane

$$H := \left\{ \lambda \in \mathbb{R}^{d^n} \mid \sum_{i=1}^{(d^n-1)/2} \lambda_i = \frac{1}{2} \right\} \quad (72)$$

with edges connecting a vertex that violates Eq. (64) to a vertex that satisfies it.

The only vertices of the Weyl chamber that are compatible with Eq. (64) are v_{d^n} (the spectrum of the maximally mixed state) and v_{d^n-1} . v_{d^n-1} lies on the hyperplane, so there are no new vertices obtained by intersecting H with line segments of the form $[v_{d^n-1}, v_k]$ for $k = 1, \dots, d^n - 2$.

Since the Weyl chamber is a simplex, all pairs of vertices Eq. (71) are connected by edges. Therefore, we need to check for intersections of H with all line segments connecting v_{d^n} to all of v_1, \dots, v_{d^n-2} . We now compute the intersections $v'_k := H \cap [v_{d^n}, v_k]$ explicitly. Parameterize the edge $[v_k, v_{d^n}]$ by $\nu_k(t) = (1-t)v_{d^n} + tv_k$, $t \in [0, 1]$. Then

$$[\nu_k(t)]_i = \begin{cases} \frac{1}{d^n} + t \left(\frac{1}{k} - \frac{1}{d^n} \right), & 1 \leq i \leq k, \\ \frac{1-t}{d^n}, & k < i \leq d^n. \end{cases} \quad (73)$$

Then we enforce the linear equation defining the hyperplane H , $\sum_{i=1}^{(d^n-1)/2} [\nu_k(t)]_i = \frac{1}{2}$, and solve for t to find the intersection point $v'_k := H \cap [v_{d^n}, v_k]$. Here we have two cases. For $k = 1, \dots, (d^n - 1)/2 - 1$, we have

$$v'_k = \left(\underbrace{\frac{k+1}{k(d^n+1)}, \dots, \frac{1}{d^n+1}}_{k \text{ times}}, \dots, \underbrace{\frac{1}{d^n+1}, \dots, \frac{1}{d^n+1}}_{d^n-k \text{ times}} \right), \quad (74)$$

and for $k = (d^n - 1)/2, \dots, d^n - 2$, we have

$$v'_k = \left(\underbrace{\frac{1}{d^n-1}, \dots, \frac{1}{d^n-1}}_{k \text{ times}}, \dots, \underbrace{\frac{d^n-1-k}{(d^n-1)(d^n-k)}, \dots, \frac{1}{d^n-1}}_{d^n-k \text{ times}} \right), \quad (75)$$

To summarize, the vertices of the polytope of allowed ordered spectra of AWP states are $(v'_1, \dots, v'_{d^n-2}, v_{d^n-1}, v_{d^n})$, where v'_k takes the form

Eq. (74) or Eq. (75) depending on whether $k < (d^n - 1)/2$. The set of all (unordered) spectra of AWP states is the polytope formed from the convex hull of these vertices and all of their coordinate permutations. Now we show that after allowing coordinate permutations, all of these vertices except v'_1 and v_{d^n-1} are redundant.

For $k = 1$, we have

$$v'_1 := \left(\frac{2}{d^n+1}, \underbrace{\frac{1}{d^n+1}, \dots, \frac{1}{d^n+1}}_{d^n-1 \text{ times}} \right). \quad (76)$$

Let $v_1^{(j)}$ denote the coordinate permutation of v'_1 with the entry $2/(d^n + 1)$ in position j . For $2 \leq k < (d^n - 1)/2$, let T be the set of indices of the k larger components in Eq. (74), so $|T| = k$. Then

$$v'_k = \frac{1}{|T|} \sum_{j \in T} v_1^{(j)}. \quad (77)$$

Hence, every v'_k with $2 \leq k < (d^n - 1)/2$ lies in the convex hull of permutations of v'_1 , and is redundant.

Now, for $(d^n - 1)/2 \leq k < d^n - 1$, let $T := \{k + 1, \dots, d^n\}$ be the set of indices of the smaller entries in v'_k , so $|T| = d^n - k$. For each $j \in \{1, \dots, d^n\}$ let $v_{d^n-1}^{(j)}$ be the coordinate permutation of v_{d^n-1} with a 0 in the j^{th} position. Then we can check that

$$v'_k = \frac{1}{|T|} \sum_{j \in T} v_{d^n-1}^{(j)}. \quad (78)$$

Therefore, every v'_k with $(d^n - 1)/2 \leq k \leq d^n - 2$ lies in the convex hull of the permutations of v_{d^n-1} , and so these vertices are also redundant.

Finally, note that v_d^n is also redundant after coordinate permutations, since

$$v_{d^n} = \frac{1}{d^n} \sum_{j=1}^{d^n} v_{d^n-1}^{(j)}. \quad (79)$$

Therefore, after allowing unordered spectra, all of the vertices v'_2, \dots, v'_{d^n-2} and the vertex v_{d^n} are redundant, and so the set of AWP spectral polytope is the convex hull of v'_1 and v_{d^n-1} and all of their coordinate permutations. \square

For the case, $d = 3$ and $n = 1$, v'_1 is a convex mixture of v_{d^n-1} and its coordinate permutations (in particular, $v'_1 = (v_2^{(2)} + v_2^{(3)})/2$ using the notation from the proof above), so the polytope of AWP spectra is a simplex spanned by v_2 and its coordinate permutations, but this is not true in general. For all Hilbert space dimensions larger than 3, v'_1 is not a mixture of v_{d^n} and its coordinate permutations, so the AWP spectra are a convex hull of two simplexes, one generated by v'_1 and the other generated by v_{d^n-1} .

An illustration of the set of qutrit AWP spectra is shown in Figure 4. Here we see that the AWP polytope (red) has vertices on spectra with only two non-vanishing eigenvalues equal to $\frac{1}{2}$. This implies that for qutrit states, any equal mixture of two orthogonal pure states is already absolutely Wigner-positive. More generally, Theorem 6 says there exist AWP states with rank $d^n - 1$.

Relatedly, the muggle polytope is always strictly contained in the AWP polytope, which implies the existence of mixed states that are non-stabilizer (i.e. magic) yet are absolutely Wigner-positive. This can be seen as a strengthening of the notion of bound magic introduced in [32], where it was shown that the Wigner polytope was a superset of the stabilizer polytope.

V. PURITY BOUNDS

Here we discuss the inscribed Hilbert-Schmidt ball of the stabilizer and Wigner polytopes, which amount to sufficient conditions for inclusion based on purity. We also discuss the circumradius of the Wigner polytope, which is a necessary condition. We then do a comparison to the balls of positive semi-definite matrices and absolutely separable states.

A. Inradius of the stabilizer polytope

In this section we find the inradius of the stabilizer polytope, i.e., the radius of the largest ball which is contained in the stabilizer polytope. By unitary invariance, this is also the largest ball contained in the set of absolutely stabilizer states. A state having Bloch radius less than this inradius thus acts as a tight sufficient condition for a state to be a mixture of stabilizer states, as well as being absolutely stabilizer. Conversely, this radius also characterizes the how impure magic non-stabilizer states can be. That is, there exist non-stabilizer states with Bloch radius only infinitesimally larger than the inradius of the stabilizer polytope. Interestingly, we find a drastic difference between the inradius of the stabilizer polytope for even versus odd qudit dimension d .

For a polytope P , let $r(P)$ denote the inradius of P , i.e., the radius of the largest ball of the same dimension as P which is contained in P . Similarly, let $R(P)$ denote the circumradius of P , the radius of the smallest ball containing P . For a general polytope, a ball contained in the polytope that achieves the inradius is not necessarily centred at the origin. Therefore, to start, we need the following lemma.

Lemma 4. *The stabilizer polytope contains a $d^{2n} - 1$ -dimensional ball of radius $r(\text{STAB}_0)$ centred at the maximally mixed state.*

Proof of Lemma 4. It suffices to show that STAB_0 contains a $d^{2n} - 1$ -dimensional ball of radius $r(\text{STAB}_0)$ which is centred at the origin in $\text{Herm}_0(\mathcal{H})$, i.e., the zero operator $\mathbb{0}$.

Let $B(c, r)$ denote a ball of radius r centred at c . By definition of $r(\text{STAB}_0)$, STAB_0 contains a ball of radius $r(\text{STAB}_0)$. Let $B(A, r(\text{STAB}_0)) = A + B(\mathbb{0}, r(\text{STAB}_0))$ be such a ball. If $A = \mathbb{0}$, then we are done. If $A \neq \mathbb{0}$, then consider the action of the Clifford group on this ball. We get an orbit of balls,

$$\left\{ g(A + B(\mathbb{0}, r(\text{STAB}_0)))g^\dagger \mid g \in \mathcal{C}\ell \right\}. \quad (80)$$

Since the stabilizer polytope is closed under the action of the Clifford group, each of these balls is contained in STAB_0 .

By convexity, the stabilizer polytope also contains a uniform mixture of these balls with respect to the Minkowski sum,

$$\frac{1}{|\mathcal{C}\ell|} \sum_{g \in \mathcal{C}\ell} g(A + B(\mathbb{0}, r(\text{STAB}_0)))g^\dagger \subset \text{STAB}_0. \quad (81)$$

But since conjugation by unitaries preserves the Hilbert-Schmidt inner product,

$$gB(\mathbb{0}, r(\text{STAB}_0))g^\dagger = B(\mathbb{0}, r(\text{STAB}_0)), \quad \forall g \in \mathcal{C}\ell. \quad (82)$$

Further, the Clifford group on prime dimensional qudits is always a unitary 2-design [54], and for qubits it is a unitary 3-design [55, 56], so

$$\frac{1}{|\mathcal{C}\ell|} \sum_{g \in \mathcal{C}\ell} g(A + B(\mathbb{0}, r(\text{STAB}_0)))g^\dagger \quad (83)$$

$$= \left[\frac{1}{|\mathcal{C}\ell|} \sum_{g \in \mathcal{C}\ell} gAg^\dagger \right] + B(\mathbb{0}, r(\text{STAB}_0)) \quad (84)$$

$$= B(\mathbb{0}, r(\text{STAB}_0)) \subset \text{STAB}_0. \quad (85)$$

This completes the proof. \square

Essentially the same argument shows that Λ is contained in $d^{2n} - 1$ -dimensional ball of radius $R(\Lambda_0)$ which is centred at the maximally mixed state. To find the inradius of the stabilizer polytope, we use the following lemma, a variant of one of the cases in Ref. [57, §1.2].

Lemma 5. *Let P be a polytope. If P contains a ball of radius $r(P)$ centred at the origin, and P° is contained in a ball of radius $R(P^\circ)$ centred at the origin, then $r(P)R(P^\circ) = 1$.*

Proof of Lemma 5. Let $B := B(\mathbb{0}, 1)$, $r := r(P)$, and $R := R(P^\circ)$. By assumption, $rB \subseteq P$ and $P^\circ \subseteq RB$. We use three facts about polarity [48, 58]: (1) taking polar duals reverses inclusions, (2) since P contains the origin, $(P^\circ)^\circ = P$, and (3) for any $t > 0$, $(tB)^\circ = \frac{1}{t}B$. Then, we have

$$P^\circ \subseteq (rB)^\circ = \frac{1}{r}B \quad (86)$$

and

$$\frac{1}{R}B = (RB)^\circ \subseteq (P^\circ)^\circ = P. \quad (87)$$

Therefore, $R \leq \frac{1}{r}$ and $r \geq \frac{1}{R}$, so $rR = 1$. \square

Using this Lemma 5, our strategy for finding the inradius of the multiqubit stabilizer polytope proceeds in two steps. First, we relate the inradius of STAB_0 to the circumradius of Λ_0 via $r(\text{STAB}_0) = 1/R(\Lambda_0)$, and second we find the circumradius of Λ_0 . Since the vertices of the Λ polytopes have a different structure for $d = 2$ versus odd-prime d , here we split into two cases.

1. Qubits

The following result gives us a bound on the inradius.

Lemma 6. *For any CNC operator A_Ω^γ , we have*

$$\text{Tr}(A_\Omega^{\gamma^2}) = \frac{|\Omega|}{d^n}. \quad (88)$$

Proof of lemma 6. By direct calculation we obtain

$$\begin{aligned} \text{Tr}(A_\Omega^{\gamma^2}) &= \text{Tr}(A_\Omega^{\gamma\dagger} A_\Omega^\gamma) \\ &= \frac{1}{d^{2n}} \sum_{a,b \in \Omega} \omega^{\gamma(a) - \gamma(b)} \text{Tr}(T_a^\dagger T_b) \\ &= \frac{1}{d^n} \sum_{a,b \in \Omega} \omega^{\gamma(a) - \gamma(b)} \delta_{a,b} \\ &= \frac{1}{d^n} \sum_{a \in \Omega} 1 = \frac{|\Omega|}{d^n}. \end{aligned} \quad (89)$$

In the first line we use the fact that CNC operators are Hermitian [22, 44], in the second line we use the definition of CNC operators Eq. (22), and the third line we use the orthogonality of Pauli operators, $\text{Tr}(T_a^\dagger T_b) = d^n \delta_{a,b}$. \square

Using the classification of CNC sets Theorem 1, we can see that the size of a maximal CNC set of the form Eq. (23) with parameters m is $|\Omega| = (2m + 2)2^{n-m}$. Therefore, among CNC operators A_Ω^γ , the value $\text{Tr}(A_\Omega^{\gamma^2})$ is maximized for the case $m = 1$, with $\text{Tr}(A_\Omega^{\gamma^2}) = 2$.

We make the following conjecture.

Conjecture 2. *For any number of qubits, for any $X \in \text{Herm}_1(\mathcal{H})$, if $\text{Tr}(X^2) > 2$ then $X \notin \Lambda$.*

In Appendix A, we show that this conjecture holds for $n = 1$ and $n = 2$, and we provide evidence that it holds generally. Now, with the following theorem, we find a formula for the inradius of the stabilizer polytope conditional on Conjecture 2.

Theorem 7. *If Conjecture 2 is true, then the Hilbert-Schmidt inradius of the n -qubit stabilizer polytope is*

$$r(\text{ASTAB}_0) = r(\text{STAB}_0) = \frac{1}{\sqrt{2^n(2^{n+1} - 1)}}. \quad (90)$$

Proof of Theorem 7. The first equality holds by unitary invariance. Assuming Conjecture 2 is true, we have $\max_{X \in \Lambda} \text{Tr}(X^2) = 2$, or equivalently,

$$R(\Lambda_0) = \sqrt{\max_{X_0 \in \Lambda_0} \text{Tr}(X_0^2)} = \sqrt{2 - \frac{1}{2^n}}. \quad (91)$$

Therefore,

$$R(-2^n \Lambda_0) = 2^n R(\Lambda_0) = \sqrt{2^n(2^{n+1} - 1)}. \quad (92)$$

Then using Lemma 5 and using polar duality of STAB_0 and $-2^n \Lambda_0$, the result follows. \square

Corollary 3. *Assuming Conjecture 2 is true, then every state ρ with purity*

$$\text{Tr}(\rho^2) \leq \frac{1}{2^n} + \frac{1}{2^n(2^{n+1} - 1)} = \frac{1}{2^n - \frac{1}{2}} \quad (93)$$

is a mixture of stabilizer states.

This corollary demonstrates that our Conjecture 2 is equivalent to Conjecture 1 in Ref. [17], which constructed a PPT-like analog for the resource theory of magic. This connection offers an additional geometric interpretation (conditioned on the validity of our conjecture) of the purity in Ref. [17] as corresponding to the inradius of the stabilizer polytope.

2. Odd-prime-dimensional qudits

The structure of the argument is similar in the case of odd-prime-dimensional qudits, the main difference is that in this case, we know that the vertices of Λ with the largest Hilbert-Schmidt norm are the phase space point operators of the Wigner function [21, 30, 46]. This gives us the following (unconditional) theorem.

Theorem 8. *For any number of qudits n of any odd-prime dimension d , the Hilbert-Schmidt inradius of the n -qudit stabilizer polytope is*

$$r(\text{ASTAB}_0) = r(\text{STAB}_0) = \frac{1}{\sqrt{d^n(d^{2n} - 1)}}. \quad (94)$$

Proof of Theorem 8. The first equality holds by unitary invariance. Phase space point operators of the Wigner function are vertices of Λ [21]. They are CNC-type operators, A_Ω^γ , with $\Omega = \mathbb{Z}_d^{2n}$ and $\gamma : \mathbb{Z}_d^{2n} \rightarrow \mathbb{Z}_d$ a linear function. By Lemma 6, these operators have

$$\text{Tr}(A_{\mathbb{Z}_d^{2n}}^{\gamma^2}) = \frac{|\mathbb{Z}_d^{2n}|}{d^n} = d^n. \quad (95)$$

With Lemma 3 from Ref. [21], coefficients of the Pauli basis expansion for any vertex A_α of Λ satisfy

$$|\mathrm{Tr}(T_a A_\alpha)| \leq 1, \quad \forall a \in \mathbb{Z}_d^{2n}. \quad (96)$$

Therefore,

$$\mathrm{Tr}(A_\alpha^2) = \frac{1}{d^n} \sum_{v \in \mathbb{Z}_d^{2n}} |\mathrm{Tr}(T_v A_\alpha)|^2 \quad (97)$$

$$\leq \frac{1}{d^n} \sum_{v \in \mathbb{Z}_d^{2n}} |\mathrm{Tr}(T_v A_\alpha)| \leq d^n. \quad (98)$$

That is, no vertex A_α of Λ can have $\mathrm{Tr}(A_\alpha^2) > d^n$, and so $\max_{X \in \Lambda} \mathrm{Tr}(X^2) = d^n$.

Equivalently,

$$R(\Lambda_0) = \sqrt{\max_{X_0 \in \Lambda_0} \mathrm{Tr}(X_0^2)} = \sqrt{d^n - \frac{1}{d^n}} \quad (99)$$

Therefore,

$$R(-d^n \Lambda_0) = d^n R(\Lambda_0) = \sqrt{d^n(d^{2n} - 1)}. \quad (100)$$

Finally, using Lemma 5 and polar duality of STAB_0 and $-d^n \Lambda_0$, we get the stated result. \square

Corollary 4. *Every state ρ with purity*

$$\mathrm{Tr}(\rho^2) \leq \frac{1}{d^n} + \frac{1}{d^n(d^{2n} - 1)} = \frac{1}{d^n - \frac{1}{d^n}} \quad (101)$$

is a mixture of stabilizer states.

B. Inradius and circumradius of AWP states

Using similar methods as above, we can get the inradius of the Wigner polytope.

Theorem 9. *For any number of qudits n of any odd-prime Hilbert space dimension d , the Hilbert-Schmidt inradius of WP_0 and AWP_0 is*

$$r(\mathrm{AWP}_0) = r(\mathrm{WP}_0) = \frac{1}{\sqrt{d^n(d^{2n} - 1)}}, \quad (102)$$

and the circumradius of AWP_0 is

$$R(\mathrm{AWP}_0) = \frac{1}{\sqrt{d^n(d^n - 1)}}. \quad (103)$$

Proof of Theorem 9. The Wigner function is Clifford covariant [25, 30, 46]. Therefore, the Wigner polytope is closed under the action of the Clifford group, and so using the same argument as in the proof of Lemma 4, we can assume that the ball contained in the Wigner polytope that achieves the inradius is centred at the maximally mixed state, or equivalently, the ball contained in WP_0 that achieves the inradius is centred at 0.

Then the proof of the first statement (inradius) is essentially the same as the proof of Theorem 8, except the Wigner polytope and its dual each have only one unitary group orbit of vertices, and they're both proportional to phase space point operators.

For the second statement (circumradius), by unitary invariance of the ball centred at the maximally mixed state with radius $R(\mathrm{AWP}_0)$, it suffices to find the largest possible Hilbert-Schmidt distance from the maximally mixed state to a diagonal AWP state. The possible entries of a diagonal AWP state forms a polytope characterized in Theorem 6. The vertices of this polytope have diagonal entries of the form Eq. (65). The Hilbert-Schmidt distance from the maximally mixed state to the first of these vertices is

$$\left\| v_{d^n-1} - \left(\frac{1}{d^n}, \frac{1}{d^n}, \dots \right) \right\|_2 = \frac{1}{\sqrt{d^n(d^n - 1)}}, \quad (104)$$

and to the second of the vertices is

$$\left\| v'_1 - \left(\frac{1}{d^n}, \frac{1}{d^n}, \dots \right) \right\|_2 = \sqrt{\frac{d^n - 1}{d^n(d^n + 1)^2}}, \quad (105)$$

where v_{d^n-1} and v'_1 are defined in the proof of Theorem 6. The first value is always the larger of the two. This proves the second statement of the theorem. \square

Corollary 5. *Every state ρ with purity*

$$\mathrm{Tr}(\rho^2) \leq \frac{1}{d^n} + \frac{1}{d^n(d^{2n} - 1)} = \frac{1}{d^n - \frac{1}{d^n}} \quad (106)$$

is AWP, and every state ρ with purity

$$\mathrm{Tr}(\rho^2) > \frac{1}{d^n} + \frac{1}{d^n(d^n - 1)} = \frac{1}{d^n - 1}. \quad (107)$$

is not AWP.

That is, if $\mathrm{Tr}(\rho^2) \leq 1/(d^n - 1/d^n)$, then for every unitary $U \in \mathrm{U}(d^n)$, the Wigner function of $U\rho U^\dagger$ is non-negative, and if $\mathrm{Tr}(\rho^2) > 1/(d^n - 1)$ then there exists a unitary $U \in \mathrm{U}(d^n)$ such that the Wigner function of $U\rho U^\dagger$ takes negative values.

C. Comparison to other balls

Here we briefly compare the Hilbert-Schmidt balls derived above with other balls of interest. We emphasize that our $r(\mathrm{STAB}_0)$ for qubits relies on a conjecture, while for odd-prime-qudits it is a theorem.

In dimensions $d^n > 2$, it is no longer true that all Hermitian operators with unit Hilbert-Schmidt norm correspond to positive semi-definite (PSD) operators, i.e. quantum states. The radius of the largest inscribed ball of PSD matrices centred at the maximally mixed state $\frac{1}{d^n}\mathbb{I}$ is well-known [59, 60] to be

$$r_{\mathrm{PSD}} = \frac{1}{\sqrt{d^n(d^n - 1)}} > r(\mathrm{STAB}_0). \quad (108)$$

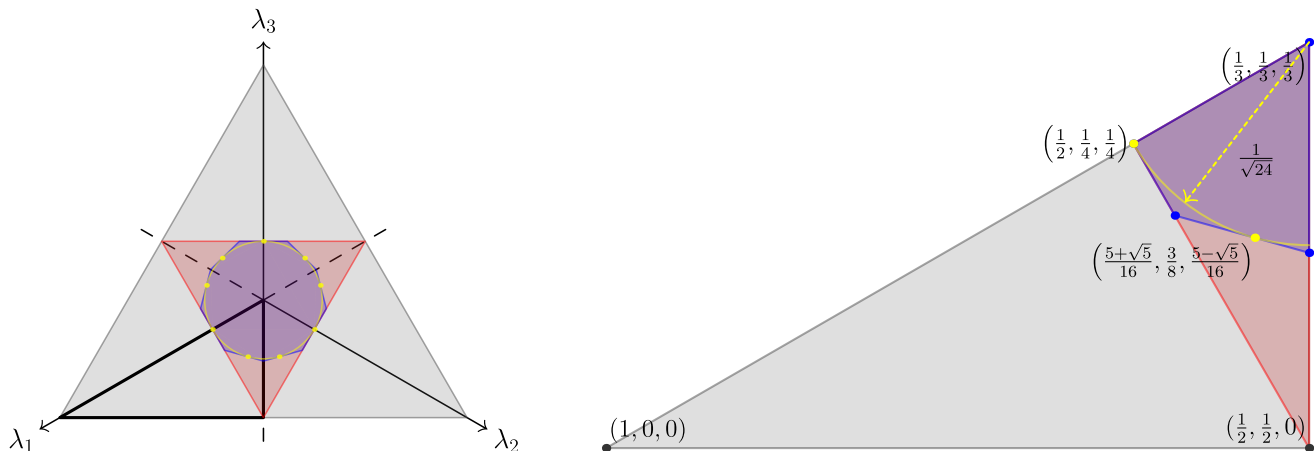


FIG. 5. Left: Ternary plot of the spectra of single-qudit absolutely stabilizer states (blue), absolutely Wigner-positive states (red), together with the inradius (yellow) common to both. Yellow dots denote absolutely stabilizer states on the boundary of both ASTAB and its inradius. Right: the associated Weyl chamber with the spectra of these special points displayed together with the Hilbert-Schmidt radius $r(\text{ASTAB}) = \frac{1}{\sqrt{24}}$.

Hence all traceless Hermitian operators within $r(\text{STAB}_0)$ can be interpreted as (shifted) quantum states. This is true regardless of d being 2 or an odd-prime, however for $d = 2$ it is notable how close the two radii are. For odd-prime dimensions, this radius exactly matches that of the circumradius of the set of absolutely Wigner-positive states (103):

$$r_{\text{PSD}} = R(\text{AWP}_0). \quad (109)$$

Hence every traceless Hermitian operator inside AWP_0 also corresponds to a valid quantum state.

Another notable ball is the Gurvits-Barnum ball of absolutely separable states, centred at the maximally mixed state [61] (see also [47]) with radius

$$r_{\text{GB}} = \frac{2}{(\sqrt{2d})^n}, \quad (110)$$

$$r(\text{ASTAB}_0) = r(\text{STAB}_0) = r(\text{AWP}_0) = r(\text{WP}_0) < r_{\text{GB}} < r_{\text{PSD}} = R(\text{AWP}_0). \quad (112)$$

Eq. (112) is to be read as follows. For odd-prime dimensions, it has been proven and does not rely on any conjectures. For $d = 2$ the Wigner polytope in the sense used in this paper is not defined, and $r(\text{STAB})$ depends on our Conjecture 2, or, equivalently, Conjecture 1 from Ref. [17]. Otherwise, the remaining relations hold.

VI. DISCUSSION

Here we characterized the set of absolutely stabilizer states for n qudits as a polytope in the simplex of state spectra. This was done by analyzing the vertices of Λ ,

where separability is defined with respect to the usual partition $(\mathbb{C}^d)^{\otimes n}$. Note that $r_{\text{GB}} < r_{\text{PSD}}$. This radius is known to be optimal in the bipartite case [62], while larger balls have been found in the multipartite case [63–65]. In comparison to the stabilizer polytope we have

$$r(\text{STAB}_0) < r_{\text{GB}}, \quad (111)$$

for all prime dimensions d . Hence all n -qudit states inside the stabilizer inscribed ball are also absolutely separable. This also immediately applies to the inscribed ball of absolutely Wigner-positive states. However, notably, since the circumradius of AWP_0 is greater than the Gurvits-Barnum ball, it is highly likely there exist entangled AWP states; see also [28].

To summarize all of the above, together with results from previous sections, we have the following chain of inclusions of Hilbert-Schmidt balls (i.e. rescaled purities):

the polar dual of the stabilizer polytope, to create a set of linear constraints on the eigenvalues of a general mixed state. Restricting to prime local dimension, we then focused on the closed and noncontextual (CNC) vertices of Λ to develop Conjecture 1 on finding a facet-minimal description of the multi-qubit muggle polytope. This conjecture essentially says that only the CNC vertices, which are a tiny subset of $\text{vert}(\Lambda)$, are required. This was explicitly proved in low-dimensional cases, and numerical evidence for its validity in larger systems was presented in the appendix. We then applied our framework to absolute Wigner positivity to introduce the AWP polytopes in the simplex of spectra. These had a simpler structure due

to the smaller number of facets to the Wigner polytope relative to the stabilizer polytope. The inradius of these balls, which amount to purity-based sufficient conditions for state inclusion, were then studied. This resulted in complete results in odd dimensions and in Conjecture 2 for qubits. We ended with a comparison to other known balls, namely those of absolute separability and positive semi-definiteness.

This work opens up several lines of future research, the most immediate of which being to advance Conjecture 1 on the sufficiency of the CNC operators in the many-qubit Λ polytope. This will require a better understanding of how the CNC polytopes (i.e. the convex hull of the CNC operators) relate to the remaining vertices. A related avenue is to explore the feasibility of this conjecture for qudits with odd-prime dimensions. This appears to be even more difficult than the qubit case due to the globally non-linear value assignments unique to this setting.

The other primary follow-up is to advance Conjecture 2 on the circumradius of Λ for qubits, or, equivalently, the inradius of the qubit stabilizer polytope. Such a result would amount to a sufficient and tight test for absolute stabilizerness based only on purity. This conjecture is moreover equivalent to Conjecture 1 of Ref. [17], where the same purity threshold is derived via the Triangle Criterion, a magic analogue of the PPT test. This suggests that the structure of the Λ polytope may provide insight to related protocols on magic state witnessing and distillation. Finding the circumradius of the set of absolutely stabilizer states is also an open problem, which would provide a tight necessary condition for absolute stabiliz-

erness. This circumradius could then be compared to the ball of absolutely separable states. If the former is bigger than the latter, this would give strong evidence towards there existing entangled absolutely stabilizer multi-qubit states. Conclusively relating entanglement to absolute stabilizerness or absolute Wigner-positivity is left open for future work.

We also mention the possibility of extending our framework to quantum channels via the Choi matrix representation [14, 15, 31, 40]. This would entail the characterization of “completely muggle-preserving” channels as those that preserve the set of absolutely stabilizer states regardless of any coupling to ancilla; see also [66]. Associated to this would be a resource theory of unitarily-accessible magic, analogous to [26, 67].

ACKNOWLEDGMENTS

We thank Ernesto Galvão and Mark Howard for insightful discussions. M.Z. is funded by the Natural Sciences and Engineering Research Council of Canada (NSERC). J.D. acknowledges funding from the European Union’s Horizon Europe Framework Programme (EIC Pathfinder Challenge project Veriqub) under Grant Agreement No. 101114899. This project grew out of discussions that took place at the Algebraic Structures in Quantum Computation Workshop (ASQC6) at Leibniz University Hannover in 2025. We thank Robert Raussendorf and the rest of the organizing committee for the invitation.

-
- [1] D. Gottesman, *Stabilizer codes and quantum error correction*, Ph.D. thesis, California Institute of Technology (1997), [arXiv:quant-ph/9705052](#).
 - [2] D. Gottesman, in *NASA International Conference on Quantum Computing and Quantum Communications*, edited by C. P. Williams (Springer Berlin Heidelberg, Berlin, Heidelberg, 1999) pp. 302–313, [arXiv:quant-ph/9802007](#).
 - [3] S. Aaronson and D. Gottesman, *Physical Review A* **70**, 052328 (2004), [arXiv:quant-ph/0406196](#).
 - [4] E. T. Campbell and D. E. Browne, On the Structure of Protocols for Magic State Distillation, in *Theory of Quantum Computation, Communication, and Cryptography*, edited by A. Childs and M. Mosca (Springer Berlin Heidelberg, Berlin, Heidelberg, 2009) pp. 20–32, [arXiv:0908.0838](#).
 - [5] S. Bravyi, G. Smith, and J. A. Smolin, *Physical Review X* **6**, 021043 (2016), [arXiv:1506.01396](#).
 - [6] S. Bravyi and D. Gosset, *Physical Review Letters* **116**, 250501 (2016), [arXiv:1601.07601](#).
 - [7] S. Bravyi, D. Browne, P. Calpin, E. Campbell, D. Gosset, and M. Howard, *Quantum* **3**, 181 (2019), [arXiv:1808.00128](#).
 - [8] J. R. Seddon, B. Regula, H. Pashayan, Y. Ouyang, and E. T. Campbell, *PRX Quantum* **2**, 010345 (2021), [arXiv:2002.06181](#).
 - [9] D. Gottesman and I. L. Chuang, *Nature* **402**, 390 (1999), [arXiv:quant-ph/9908010](#).
 - [10] S. Bravyi and A. Kitaev, *Physical Review A* **71**, 022316 (2005), [arXiv:quant-ph/0403025](#).
 - [11] M. Howard, J. Wallman, V. Veitch, and J. Emerson, *Nature* **510**, 351 (2014), [arXiv:1401.4174](#).
 - [12] V. Veitch, S. H. Mousavian, D. Gottesman, and J. Emerson, *New Journal of Physics* **16**, 013009 (2014), [arXiv:1307.7171](#).
 - [13] M. Howard and E. Campbell, *Physical Review Letters* **118**, 090501 (2017), [arXiv:1609.07488](#).
 - [14] J. R. Seddon and E. T. Campbell, *Proceedings of the Royal Society A* **475**, 20190251 (2019), [arXiv:1901.03322](#).
 - [15] A. Heimendahl, M. Heinrich, and D. Gross, *Journal of Mathematical Physics* **63**, 112201 (2022), [arXiv:2011.11651](#).
 - [16] B. Eastin and E. Knill, *Physical Review Letters* **102**, 110502 (2009), [arXiv:0811.4262](#).
 - [17] Z. Liu, T. Haug, Q. Ye, Z.-W. Liu, and I. Roth, A magic criterion (almost) as nice as PPT, with applications in distillation and detection (2025), [arXiv:2512.16777](#).

- [18] R. Wagner, F. C. R. Peres, E. Zambrini Cruzeiro, and E. F. Galvão, *Journal of Physics A* **58**, 285302 (2025), [arXiv:2404.16107](#).
- [19] A. Heimendahl, *The stabilizer polytope and contextuality for qubit systems*, *Master's thesis*, University of Cologne (2019).
- [20] M. Zurel, C. Okay, and R. Raussendorf, *Physical Review Letters* **125**, 260404 (2020), [arXiv:2004.01992](#).
- [21] M. Zurel, C. Okay, R. Raussendorf, and A. Heimendahl, *Quantum* **8**, 1323 (2024), [arXiv:2110.12318](#).
- [22] R. Raussendorf, J. Bermejo-Vega, E. Tyhurst, C. Okay, and M. Zurel, *Physical Review A* **101**, 012350 (2020), [arXiv:1905.05374](#).
- [23] N. D. Mermin, *Reviews of Modern Physics* **65**, 803 (1993), [arXiv:1802.10119](#).
- [24] C. Okay, S. Roberts, S. D. Bartlett, and R. Raussendorf, *Quantum Information and Computation* **17**, 1135 (2017), [arXiv:1701.01888](#).
- [25] R. Raussendorf, C. Okay, M. Zurel, and P. Feldmann, *Quantum* **7**, 979 (2023), [arXiv:2110.11631](#).
- [26] R. Salazar, J. Czartowski, and A. de Oliveira Junior, *Resource theory of Absolute Negativity* (2022), [arXiv:2205.13480](#).
- [27] V. Abgaryan, A. Khvedelidze, and A. Torosyan, *Journal of Mathematical Sciences* **251**, 301 (2020), [arXiv:1910.11220](#).
- [28] J. Denis, J. Davis, R. B. Mann, and J. Martin, *Quantum* **8**, 1550 (2024), [arXiv:2304.09006](#).
- [29] W. K. Wootters, *Annals of Physics* **176**, 1 (1987).
- [30] D. Gross, *Journal of Mathematical Physics* **47**, 122107 (2006), [arXiv:quant-ph/0602001](#).
- [31] X. Wang, M. M. Wilde, and Y. Su, *New Journal of Physics* **21**, 103002 (2019), [arXiv:1903.04483](#).
- [32] V. Veitch, C. Ferrie, D. Gross, and J. Emerson, *New Journal of Physics* **14**, 113011 (2012), [arXiv:1201.1256](#).
- [33] E. T. Campbell and D. E. Browne, *Physical Review Letters* **104**, 030503 (2010), [arXiv:0908.0836](#).
- [34] S. Prakash and A. Gupta, *Physical Review A* **101**, 010303 (2020), [arXiv:1905.00392](#).
- [35] D. M. Appleby, *Journal of Mathematical Physics* **46**, 052107 (2005), [arXiv:quant-ph/0412001](#).
- [36] N. D. Beaudrap, *Quantum Information and Computation* **13**, 73 (2013), [arXiv:1102.3354](#).
- [37] D. Gross and M. Walter, *Journal of Mathematical Physics* **54**, 082201 (2013), [arXiv:1302.6990](#).
- [38] T. Singal, C. Chiang, E. Hsu, E. Kim, H.-S. Goan, and M.-H. Hsieh, *Quantum* **7**, 1048 (2023), [arXiv:2209.01449](#).
- [39] B. W. Reichardt, *Quantum Information and Computation* **9**, 1030 (2009), [arXiv:quant-ph/0608085](#).
- [40] A. Mari and J. Eisert, *Physical Review Letters* **109**, 230503 (2012), [arXiv:1208.3660](#).
- [41] H. Pashayan, J. J. Wallman, and S. D. Bartlett, *Physical Review Letters* **115**, 070501 (2015), [arXiv:1503.07525](#).
- [42] N. Delfosse, C. Okay, J. Bermejo-Vega, D. E. Browne, and R. Raussendorf, *New Journal of Physics* **19**, 123024 (2017), [arXiv:1610.07093](#).
- [43] B. Kim and S. Abramsky, *State-independent all-versus-nothing arguments* (2023), [arXiv:2311.11218](#).
- [44] M. Zurel and A. Heimendahl, *Efficient classical simulation of quantum computation beyond Wigner positivity* (2024), [arXiv:2407.10349](#).
- [45] A. Y. M. Chin, *Journal of group theory* **8**, 189 (2005).
- [46] D. Gross, *Computational power of quantum many-body states and some results on discrete phase spaces*, *Ph.D. thesis*, Imperial College London (2008).
- [47] M. Kus and K. Życzkowski, *Physical Review A* **63**, 032307 (2001), [arXiv:quant-ph/0006068](#).
- [48] G. M. Ziegler, *Lectures on Polytopes* (Springer, New York, 1995).
- [49] K. Fan, *Proceedings of the National Academy of Sciences* **35**, 652 (1949).
- [50] K. Fan, *Proceedings of the National Academy of Sciences* **36**, 31 (1950).
- [51] A. W. Marshall, I. Olkin, and B. C. Arnold, *Inequalities: Theory of Majorization and Its Applications*, 2nd ed. (Springer, New York, 2011).
- [52] D. M. Appleby, I. Bengtsson, and S. Chaturvedi, *Journal of Mathematical Physics* **49**, 012102 (2008), [arXiv:0710.3013](#).
- [53] K. Fukuda and A. Prodon, in *Combinatorics and Computer Science*, edited by M. Deza, R. Euler, and I. Manoussakis (Springer Berlin Heidelberg, Berlin, Heidelberg, 1996) pp. 91–111.
- [54] D. Gross, K. Audenaert, and J. Eisert, *Journal of Mathematical Physics* **48**, 052104 (2007), [arXiv:quant-ph/0611002](#).
- [55] Z. Webb, *Quantum Information and Computation* **16**, 1379 (2016), [arXiv:1510.02769](#).
- [56] H. Zhu, *Physical Review A* **96**, 062336 (2017), [arXiv:1510.02619](#).
- [57] P. Gritzmann and V. Klee, *Discrete & Computational Geometry* **7**, 255 (1992).
- [58] L. Narici and E. Beckenstein, *Topological Vector Spaces* (Chapman & Hall / CRC, London, 2010).
- [59] J. E. Harriman, *Physical Review A* **17**, 1249 (1978).
- [60] I. Bengtsson and K. Życzkowski, *Geometry of Quantum States* (Cambridge University Press, Cambridge, 2006).
- [61] L. Gurvits and H. Barnum, *Physical Review A* **68**, 042312 (2003), [arXiv:quant-ph/0302102](#).
- [62] L. Gurvits and H. Barnum, *Physical Review A* **66**, 062311 (2002), [arXiv:quant-ph/0204159](#).
- [63] L. Gurvits and H. Barnum, *Physical Review A* **72**, 032322 (2005), [arXiv:quant-ph/0409095](#).
- [64] R. Hildebrand, *Physical Review A* **75**, 062330 (2007), [arXiv:quant-ph/0702040](#).
- [65] R. Y. Wen, G. Perez, L. Lyu, W. Witczak-Krempa, and A. Kempf, *Physical Review A* **112**, 012426 (2025), [arXiv:2410.05400](#).
- [66] A. Patra, R. Gupta, A. Ferraro, and A. Sen(De), *Qubit magic-breaking channels* (2024), [arXiv:2409.04425](#).
- [67] A. Patra, A. Maity, and A. Sen(De), *Physical Review A* **108**, 042402 (2023), [arXiv:2212.11105](#).

Appendix A: Evidence for Conjectures 1 and 2

We can verify Conjecture 1 and Conjecture 2 directly for $n = 1$ and $n = 2$ qubits. For $n = 1$, Λ is a cube with vertices $A_{\pm\pm\pm} = (I \pm X \pm Y \pm Z)/2$ [20]. These are all CNC operators, and so Conjecture 1 holds trivially. Also, $\text{Tr}(A_{\pm\pm\pm}^2) = 2$, and so Conjecture 2 also holds in this case.

For two qubits, we can enumerate all vertices of Λ . We find there are 22,320 vertices, which fall into 8 orbits under the action of the Clifford group with 8 distinct spectra. These spectra are listed in Table I.

Orbit	Exact eigenvalues			
CNC ($m = 1$)	$\frac{1}{2} - \frac{\sqrt{3}}{2}$	0	0	$\frac{1}{2} + \frac{\sqrt{3}}{2}$
CNC ($m = 2$)	$\frac{1}{4} - \frac{\sqrt{5}}{4}$	$\frac{1}{4} - \frac{\sqrt{5}}{4}$	$\frac{1}{4} + \frac{\sqrt{5}}{4}$	$\frac{1}{4} + \frac{\sqrt{5}}{4}$
Row 2	$-\sqrt{\frac{\sqrt{3}}{8} + \frac{15}{64} + \frac{\sqrt{3}}{8} + \frac{1}{4}}$	$-\frac{\sqrt{3}}{8} - \sqrt{\frac{15}{64} - \frac{\sqrt{3}}{8} + \frac{1}{4}}$	$-\frac{\sqrt{3}}{8} + \sqrt{\frac{15}{64} - \frac{\sqrt{3}}{8} + \frac{1}{4}}$	$\frac{\sqrt{3}}{8} + \frac{1}{4} + \sqrt{\frac{\sqrt{3}}{8} + \frac{15}{64}}$
Row 3	$-\sqrt{\frac{\sqrt{2}}{8} + \frac{7}{32} + \frac{\sqrt{2}}{8} + \frac{1}{4}}$	$-\sqrt{\frac{7}{32} - \frac{\sqrt{2}}{8} - \frac{\sqrt{2}}{8} + \frac{1}{4}}$	$-\frac{\sqrt{2}}{8} + \sqrt{\frac{7}{32} - \frac{\sqrt{2}}{8} + \frac{1}{4}}$	$\frac{\sqrt{2}}{8} + \frac{1}{4} + \sqrt{\frac{\sqrt{2}}{8} + \frac{7}{32}}$
Row 4	$\frac{1}{2} - \frac{\sqrt{7}}{4}$	0	0	$\frac{1}{2} + \frac{\sqrt{7}}{4}$
Row 5	$-\frac{\sqrt{2}\sqrt{5-\sqrt{5}}}{8} + \frac{1}{4}$	$\frac{1}{4} + \frac{\sqrt{2}\sqrt{5-\sqrt{5}}}{8}$	$-\frac{\sqrt{2}\sqrt{5+\sqrt{5}}}{8} + \frac{1}{4}$	$\frac{1}{4} + \frac{\sqrt{2}\sqrt{5+\sqrt{5}}}{8}$
Row 6	$\frac{1}{2} - \frac{\sqrt{15}}{6}$	0	0	$\frac{1}{2} + \frac{\sqrt{15}}{6}$
Row 7	$-\sqrt{\frac{11\sqrt{5}}{128} + \frac{25}{128} + \frac{1}{4} + \frac{\sqrt{5}}{8}}$	$-\frac{\sqrt{5}}{8} - \sqrt{\frac{25}{128} - \frac{11\sqrt{5}}{128} + \frac{1}{4}}$	$-\frac{\sqrt{5}}{8} + \sqrt{\frac{25}{128} - \frac{11\sqrt{5}}{128} + \frac{1}{4}}$	$\frac{1}{4} + \frac{\sqrt{5}}{8} + \sqrt{\frac{11\sqrt{5}}{128} + \frac{25}{128}}$
Orbit	Approximate decimal expansions			
CNC ($m = 1$)	-0.36603	0.00000	0.00000	1.36603
CNC ($m = 2$)	-0.30902	-0.30902	0.80902	0.80902
Row 2	-0.20497	-0.10018	0.16717	1.13798
Row 3	-0.20213	-0.13165	0.27810	1.05569
Row 4	-0.16144	0.00000	0.00000	1.16144
Row 5	-0.22553	-0.04389	0.54389	0.72553
Row 6	-0.14550	0.00000	0.00000	1.14550
Row 7	-0.09297	-0.08564	0.02662	1.15198

TABLE I. Eigenvalues of the eight unitary group orbits (or Clifford group orbits) of the vertices of the 2-qubit Λ polytope. The first two rows are the CNC-type vertices with parameters $m = 1$ and $m = 2$ according to the classification of Theorem 1. The remaining rows are labeled according to the row in which they appear in Table 2 of Ref. [39].

The partial sums, $\sum_{\ell=0}^k \lambda_{\ell}^{\downarrow}(A_{\Omega}^{\lambda})$, of the two-qubit CNC operators are plotted in Figure 6, along with the corresponding partial sums of eigenvalues, $\sum_{\ell=0}^k \lambda_{\ell}^{\downarrow}(A_{\alpha})$ of the remaining two-qubit Λ -polytope vertex spectra. From this plot we can see that all non-CNC spectra are majorized by the CNC spectrum with parameter $m = 1$. Therefore, Conjecture 1 holds for $n = 2$.

The squares of the Hilbert-Schmidt norms of these orbits are listed in Table II. Here we can see that the largest Hilbert-Schmidt norm is achieved by the CNC-type orbit of Λ -polytope vertices with parameter $m = 1$. Therefore, Conjecture 2 also holds for $n = 2$.

Orbit	$\text{Tr}(A_{\alpha}^2)$
CNC ($m = 1$)	2.0
CNC ($m = 2$)	1.5
Row 2	1.375
Row 3	1.25
Row 4	1.375
Row 5	0.875
Row 6	1.3
Row 7	1.34375

TABLE II. The square of the Hilbert-Schmidt norm $\text{Tr}(A_{\alpha}^2)$ of vertices A_{α} of the 2-qubit Λ polytope. The first two rows are CNC-type vertices. In the remaining rows, the label ‘‘Row X’’ refers to the rows in which they appear in Table II of Ref. [39].

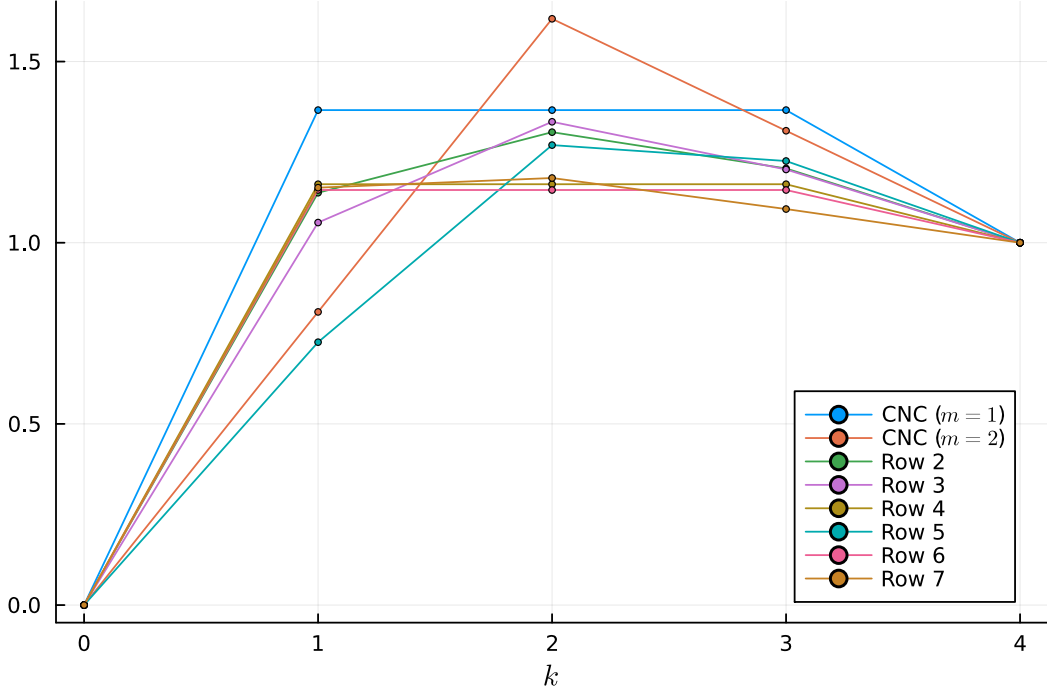


FIG. 6. Lorenz curves, $S(k|\alpha) := \sum_{\ell=1}^k \lambda_{\ell}^{\downarrow}(A_{\alpha})$, of the spectra of two-qubit Λ polytope vertices A_{α} . The first two lines correspond to the eigenvalues of the type $m = 1$ and $m = 2$ CNC type vertices. The remaining lines are the spectra of the remaining six Clifford group orbits of 2-qubit Λ polytope vertices. The legend refers to the rows of Table 2 in Ref. [39].

For $n = 3$, a complete enumeration of vertices of Λ is out of reach. We can gain evidence for the conjectures by generating random vertices of Λ and checking that they satisfy the conjectures. We can generate random vertices of Λ by choosing a random pure quantum state $|\psi\rangle$ and solving the linear program

$$\max\{\text{Tr}(|\psi\rangle\langle\psi|X) \mid X \in \Lambda\} \quad (\text{A1})$$

By the fundamental theorem of linear programming, the optimal value of this program will be achieved at a vertex of the feasible set, namely, Λ .

Using this method, we generated over 750,000 random 3-qubit vertices which fell into about 345,000 distinct orbits under the action of Clifford group. All of the spectra of the vertices generated are majorized by the type $m = 1$ CNC vertices, except for those of the other CNC-type vertices. Therefore, Conjecture 1 holds for all of the vertices generated. Some representative examples are shown in Figure 7. Similarly, all of the vertices generated have Hilbert-Schmidt norm less than or equal to the type $m = 1$ CNC vertices. A histogram of the Hilbert-Schmidt norm of these vertices is shown in Figure 8.

Generating 10,000 random 4-qubit vertices yielded similar results. All non-CNC vertices generated had spectra majorized by the $m = 1$ CNC spectrum, and all had Hilbert-Schmidt norm less than $\sqrt{2}$. Therefore, the conjectures hold for these randomly generated vertices.

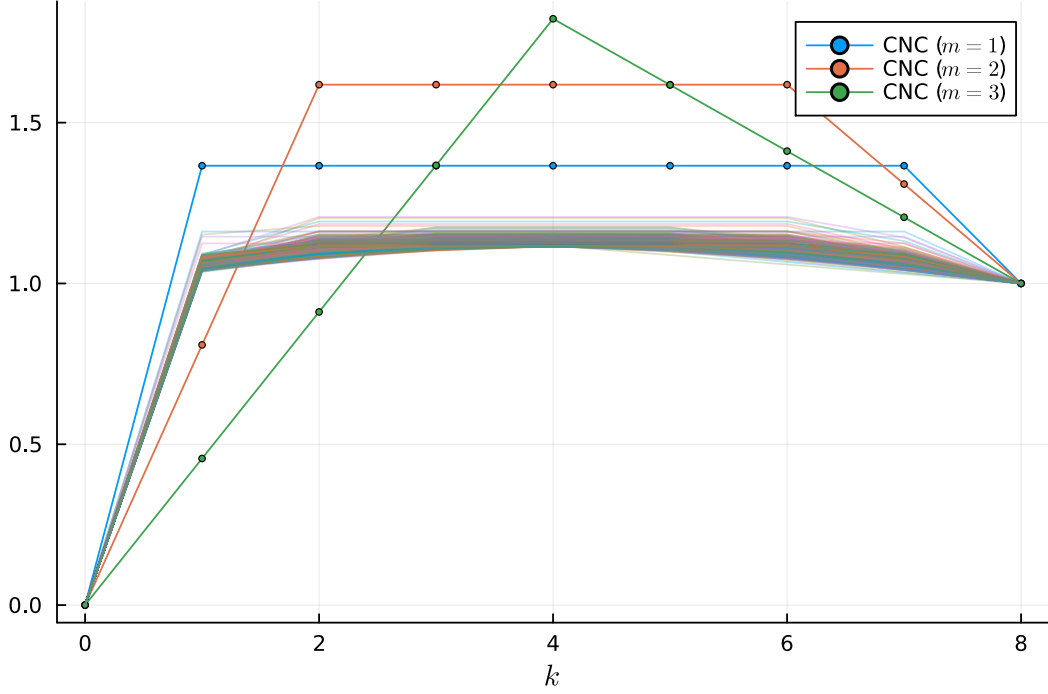


FIG. 7. Lorenz curves, $S(k|\alpha) := \sum_{\ell=1}^k \lambda_{\ell}^{\downarrow}(A_{\alpha})$, of three qubit Λ polytope vertices A_{α} . The CNC-type vertices are highlighted. Also shown are the top 1000 out of 750,000 randomly generated 3-qubit vertices that come closest to surpassing the Lorenz curve of the $m = 1$ CNC vertex.

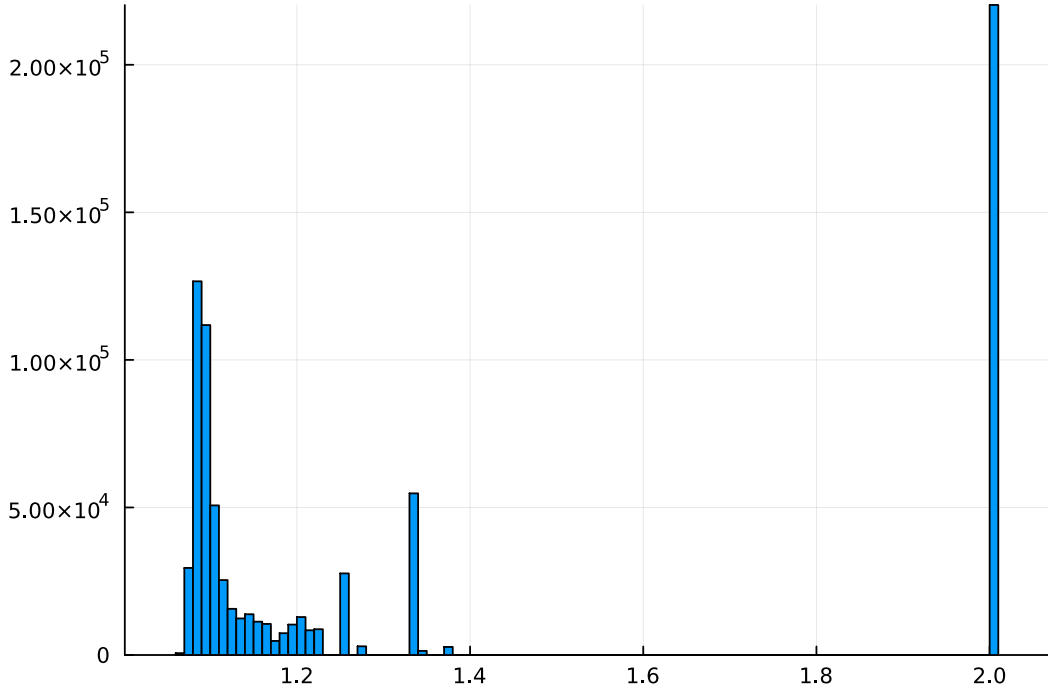


FIG. 8. Histogram showing the square of the Hilbert-Schmidt norm for 750,000 (non-unique) randomly generated vertices of the 3-qubit Λ polytope. The spike at 2 results from the fact that the method of generating random vertices of Λ is biased towards generating CNC-type vertices over the much more common non-CNC vertices.